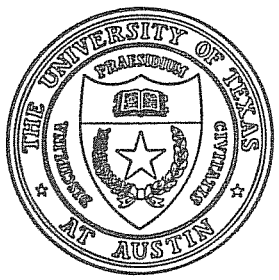

PMFSEL 90-2
DECEMBER 1990

TESTS OF HIGHLAND WAREHOUSE ROOF JOISTS

by

Michael D. Engelhardt

and

Joseph A. Yura

PHIL M. FERGUSON STRUCTURAL ENGINEERING LABORATORY
Department of Civil Engineering / Bureau of Engineering Research
The University of Texas at Austin

TESTS OF HIGHLAND WAREHOUSE ROOF JOISTS

BY

Michael D. Engelhardt

and

Joseph A. Yura

Phil M. Ferguson Structural Engineering Laboratory
Bureau of Engineering Research
The University of Texas at Austin

December 1990

SUMMARY

This report documents tests of three open web steel joists conducted in January of 1990 at The University of Texas Phil M. Ferguson Structural Engineering Laboratory in Austin, Texas. These tests were conducted at the request of Morris Engineering Company of Dallas, Texas as part of their investigation of the 1989 Highland warehouse roof collapse in Dallas. The three test joists were originally part of the warehouse roof system, and were salvaged after the roof collapse.

During testing, the joists were subject to equal point loads acting downward at each of the upper chord panel points, approximating a uniform vertical load. Two joists were tested as simply supported members. The third was tested with a lower chord extension at one end of the joist. The joists were tested to failure.

This report provides a description of the experimental setup and test procedures, a description of the behavior of each joist during testing, and data on loads, deflections and strain gage readings for each test. The maximum vertical load supported by each joist during testing is summarized in Table 3.1 on page 27 of this report.

ACKNOWLEDGEMENTS

The work described in this report was conducted at the request of Morris Engineering Company of Dallas, Texas. The assistance provided by Tom and Bill Morris in planning the test program is gratefully acknowledged. Abunnasr Husain, a graduate student in structural engineering at the University of Texas as Austin, participated throughout the test program with instrumenting the joists, assisting during the tests, and with reduction and plotting of the test data. The assistance of the Ferguson Lab staff is also acknowledged.

Contents

LIST OF FIGURES

LIST OF TABLES

1. INTRODUCTION

This report documents tests of three open web steel joists conducted in January of 1990 at The University of Texas Phil M. Ferguson Structural Engineering Laboratory in Austin, Texas. These tests were conducted at the request of Morris Engineering Company of Dallas, Texas as part of their investigation of the 1989 Highland warehouse roof collapse in Dallas. The three test joists were originally part of the warehouse roof system, and were salvaged after the roof collapse.

The objectives of these tests were to provide data on the strength, stiffness and failure mechanisms of the joists under simple and well defined support and loading conditions. An exact simulation of the actual warehouse roof system was not attempted because of the many variables and unknowns concerning the actual joist loading and support conditions at the time of the collapse. The data from this test program are intended to provide a basis for evaluating joist behavior under a variety of conditions and to provide a basis for calibrating and verifying analytical models of the roof system.

This report provides a description of the experimental setup and test procedures, a description of the behavior of each joist during testing, and data on loads, deflections and strain gage readings for each test.

2. EXPERIMENTAL SETUP AND DESCRIPTION OF TEST JOISTS

General Description of Joists

The nominal dimensions and configuration of the joists are shown in the Morris Engineering drawing reproduced in Fig. 2.1. The joists were approximately 29 ft. long and 16 inches deep. The chord members were double angles (1.5″ × 1.5″ × 3/16″ top chord; 1.5″ × 1.5″ × 1/8″ bottom chord), and the diagonals were solid round bars. The two outermost diagonals were nominally 3/4″ diameter; all other diagonals were nominally 5/8″ diameter.

In the warehouse roof system, in the region of the collapse, one end of each joist was attached to a reinforced concrete wall panel. At this end, the lower chord was extended to and attached to the wall. The other end of the joists were attached either to a joist girder or to a steel pipe column, with or without a lower chord extension.

Schematic Outline of Joist Tests

Three joists were tested to failure in this experimental program. Figure 2.2 provides a schematic representation of the three joist tests. For each test, equal point loads were applied to each of the 13 upper chord panel points. Joist Nos. 1 and 2 were tested as simply supported members, with a roller support at each end, and no lower chord extensions.

For Joist No. 3, a roller support was provided at one end. At the other end, Joist No. 3 had a lower chord extension. Connection details at this end of the joist, at both the upper and lower chords, were similar to the actual joist to wall connections in the warehouse roof system, and are described in detail later. In the description of the experimental setup that follows, the end of Joist No. 3 with the lower chord extension is referred to as the "wall end" of the joist.

Experimental Setup

Overall Setup

An overall view of the experimental setup is shown in Fig. 2.3. The ends of the test joists were supported off of W10 × 33 members which were bolted to W12 × 65 columns. The columns, in turn, were bolted to the laboratory floor. A W12 × 50 beam spanned between the W12 × 65 columns. This beam provided a reaction for the hydraulic loading rams, and supported the upper end of the joist lateral guides (described later). An additional W12 × 50 beam, bolted to the laboratory floor, supported the lower end of the joist lateral guides. Photographs of the overall setup are provided in Fig. 2.4. The north end of the test setup was intended to coincide with the wall end of Joist No. 3. (North and south directions, as referred to in this report, indicate directions in Ferguson Laboratory. They do not refer to directions at the Highland warehouse).

Joist End Supports

Details of the joist end supports are illustrated in Figs. 2.5 to 2.8. A roller support was provided at each end of Joist Nos. 1 and 2, as well as at the south end of Joist No. 3. The roller supports (Fig. 2.7), provided a vertical reaction, but offered essentially no horizontal or rotational restraint. At each roller support point, a 5/16″ thick plate was welded to the joist as shown in Fig. 2.7. This plate was provided to distribute the concentrated reaction to the joist and to avoid a local failure at the point were the roller contacted the joist. A photograph of the roller assembly is shown in Fig. 2.9. This photograph also shows a steel angle attached to the W10 × 33 with a C-clamp. This angle was provided as a safety precaution to prevent the roller assembly from slipping off the 5″ × 5″ × 1/2″ stiffened angle that supported it.

Details at the north end of Joist No. 3 are illustrated in Figs. 2.6 and 2.8. The top chord of the joist was welded to a 5″ × 5″ × 1/2″ stiffened angle, which in turn, was welded to the W10 × 33 support member. The lower chord extension at the north end of Joist No. 3 had a 3″ × 3″ × 7/32″ angle welded to its bottom. (This angle was already welded to the joist as received in Ferguson Laboratory). The angle at the end of the lower chord extension was bolted to the W10 × 33 support member. Photographs of the connection details at the north end of Joist No. 3 are provided in Fig. 2.10.

Joist Loading System

A hydraulic ram was located at each of the 13 upper chord panel points of the test joist. Each of the 13 rams were nominally identical and were connected to a common hydraulic line. The hydraulic line, in turn, was connected to a hand operated hydraulic pump. This loading system applied nominally identical downward forces at each of the 13 load points.

Figure 2.11 illustrates the details at a hydraulic ram. The rams, rated at 4 tons maximum capacity, were connected to the W12 × 50 beam. Beneath each ram, a 1/2″ steel plate was tack welded to the top of the joist in order to distribute the load to the joist. Figure 2.12 shows a photograph of the loading rams.

As described later, the joists in their initial unloaded state were not straight. Significant initial lateral displacements were measured for each joist. Prior to testing each joist, the hydraulic rams were centered over the joist at each load point. Consequently, the rams were not in a straight line, but rather conformed to the initial shape of the joist.

Joist Lateral Support System

In order to maintain the joists in a vertical position during the loading process, a lateral support system was provided. This lateral support system had two components. The first component was the joist lateral guides, provided at three locations along the joist. The joist lateral guides completely prevented lateral movement of both the upper and lower chords of the joist at the location of the guides.

Figure 2.3 shows the location of the lateral guides along the joist, which coincided with the location of lower chord bridging members in the actual roof system. Details of the lateral guides are illustrated in Fig. 2.13, and a photograph is provided in Fig. 2.14. The lateral guides are also visible in the photographs in Fig. 2.4. Although the lateral guides prevented lateral movement of the chord members, they provided essentially no restraint to vertical movement of the joist. This was accomplished by providing teflon sliding surfaces (Fig. 2.13).

The second component of the joist lateral support system was provided by friction between the head of the loading rams and the 1/2″ plates tack welded to the joist (Fig. 2.11). Because of this friction, the rams themselves restrained lateral movement of the joist's upper chord at each load point. The turnbuckles provided on each side of the rams, as shown in Fig. 2.11, restrained lateral movement of the rams. The effectiveness of friction at the loading ram in providing lateral restraint was assessed in each test by monitoring lateral movement of the joist throughout the test. These measurements, presented later in this report, indicated only slight lateral displacement of the joists. These measurements indicate that a high degree of lateral restraint was present at the upper chord of the joist at each load point. It should also be noted that none of the three test joists failed by instability of the upper chord, indicating adequate lateral restraint was provided.

In summary, the upper chord of the test joists were laterally restrained at each load point (i. e. at the panel points), as well as at the locations of the three lateral guides. The lower chord was laterally restrained only at the three lateral guides. The system was designed to reasonably simulate the lateral restraint provided to the joists by the decking and bridging in the Highland warehouse.

Instrumentation

Load

As noted earlier, the joists were loaded by 13 nominally identical hydraulic rams, at the 13 upper chord panel points. The force at each ram can be computed as the piston area of the ram multiplied by the hydraulic oil pressure acting on that area. All 13 rams were connected to a common hydraulic line, resulting in the same oil pressure at each ram. Consequently, the load at each ram was nominally the same throughout the entire loading process. Even though the extension of the rams varied as the joists deflected downward, the load remained the same at each ram.

Prior to the joist tests, each ram was calibrated in a test machine to establish the relationship between load on the ram and the oil pressure in the ram. This calibration indicated that the 13 rams produced essentially identical loads at the same oil pressure. (Loads varied by less than 3 percent among the rams).

During the tests, the oil pressure was measured by an electronic pressure transducer. This data was then converted to load readings using the individual ram calibrations noted above. The total load on the joist, as presented in the plots in Chapter 3 of this report, was

obtained by summing the 13 individual ram loads. It is estimated that the total load on the joist is accurate within approximately ± 100 lbs. In addition to the electronic pressure transducer, oil pressure was monitored with a mechanical oil pressure gage. These readings were used to control the rate of loading during the tests, and also served as a check on the electronic pressure readings.

In addition to measuring the vertical downward load applied to the joists, the vertical upward reaction was also measured at the south end (simply supported end) of Joist No. 3. This was accomplished by locating an electronic load cell underneath the roller bearing assembly. This measurement was made because Joist No. 3 was statically indeterminate, and the reaction could therefore not be determined from static equilibrium alone.

Displacement

The vertical displacement of each joist was monitored at three locations along the upper chord, as indicated in Fig. 2.15. Displacements were measured using electronic displacement transducers. One transducer was located at the third panel point from the south end, one at the center panel point, and one at the third panel point from the north end of the joist. Each transducer was actually located approximately 4 inches south of the panel point to avoid interference with the loading rams. It is estimated that the electronic displacement transducers were accurate to approximately ± .01 inches.

Displacements were also measured at the center panel point with a mechanical displacement dial gage. The dial gage readings served as a check on the electronic displacement readings.

Strain Gages

Selected members on Joist Nos. 2 and 3 were instrumented with electrical resistance strain gages in an attempt to ascertain the axial force in the members during the tests. The members that were strain gaged are indicated in Fig. 2.15. For Joist No. 2, the first compression diagonal at each end was gaged, as well as a top chord and bottom chord member near midspan. For Joist No. 3, gaged members included the first compression diagonal at each end, additional diagonal members at the north end of the joist, a top chord member near midspan, and the bottom chord extension.

The layout of strain gages for diagonals and chord members are shown in Fig. 2.16. A cluster of 4 gages was attached to each diagonal, and a cluster of 10 gages was attached to each chord member. In all cases, the gages were located at midlength of the member, and all gages were oriented longitudinally along the member. The layout of gages shown in Fig. 2.16 was chosen so that the average axial strain in the member could be computed from the individual strain gage readings. Analysis of the strain gage data is discussed in Chapter 4.

Data Collection

For each of the three joist tests, all electronic data were recorded on a computerized data acquisition system. This included pressure transducer readings (for monitoring load on the joist), displacement transducer readings, load cell readings (Joist No. 3 only), and strain gage readings (Joist Nos. 2 and 3 only). Electronic data were read on the data acquisition system at selected intervals throughout each test.

In addition to the electronic data reading described above, measurements of lateral displacements of the joists were taken during each test. To take these measurements, a transit was set up near the joist, and a line of sight was established that was approximately parallel to the joist. The distance from the line of sight to points on the joist were then read by holding a scale against the joist and reading the scale with the transit. Such readings were taken at selected locations along the joist, both before the test and at intervals during the test. These reading provided an indication of initial crookedness of the joist and also an indication of lateral movement of selected points along the joist throughout the course of each test. These data are presented in Chapter 4.

Condition of Joists Prior to Testing

The three test joists were salvaged from the Highland warehouse roof system after the collapse. The joists were delivered to Ferguson Laboratory on December 8, 1989. As delivered, all three joists showed significant damage. Photographs of each joist, as received at Ferguson Lab, are provided in Fig. 2.17. Overall, Joist No. 1 appeared to be most damaged, and Joist No. 3 appeared to be least damaged.

As can be seen in the photographs, each of the joists were laterally bent out of shape. Most of this deformation was concentrated at the joist ends. The lower chord extensions were severely damaged on Joist Nos. 1 and 2. In addition to the overall deformations, the individual angles in the chord members were twisted at several locations. No severe deformations, with the exceptions noted below, were observed in the diagonals.

As received, the joists were too deformed for testing. The large lateral deformations did not permit the joists to fit within the test setup. Further, testing of a severely distorted joist could not be expected to provide a meaningful representation of the strength or controlling failure mode of an undamaged joist. For these reasons, limited repairs were undertaken on the joists prior to testing. First, the severely distorted lower chord extensions were cut off of Joist Nos. 1 and 2. An attempt was then made to straighten out each of the joists by applying out of plane forces to the joists. In some cases, individual members were heated with a torch to facilitate straightening. Although this operation straightened out the joists by removing the largest lateral deformations, the joists still showed significant lateral distortions. It was not possible to completely straighten the joists prior to testing. The three lateral guides within the test frame were used to further straighten the joists.

Joist Nos. 1 and 2 each had one slightly bent diagonal member near midspan. Joist No. 3 also had one slightly bent diagonal at its north end. These damaged diagonals were

out-of-straight by approximately 1/4" at midlength. By virtue of their position within the joists, none of the bent diagonal members were expected to carry large forces during the tests. Consequently, no attempt was made to straighten out these bent diagonals.

After the straightening operation was completed on Joist No. 1, several broken welds were observed in the joist. These broken welds were at the north end of the joist, at the locations indicated in Fig. 2.18. It is not known when these welds were broken. It is noted, however, that the broken welds were in a severely distorted region of the joist. This region was subject to large lateral forces during the straightening of the joist. It is therefore possible that the welds were broken while straightening the joist. One of the broken welds between the diagonals and the top chord was deemed critical to the joist's load carrying capacity. Consequently, the broken welds indicated in Fig. 2.18 were repaired prior to testing of the joist.

A broken weld was also observed in Joist No. 2, also after the straightening operation was completed. This broken weld was at an intermediate connector in the top chord, near midspan. This weld was not repaired prior to testing. Based on the observed behavior of Joist No. 2 during testing (described in Chapter 3), this broken weld had no effect on the joist.

After Joist No. 1 was installed in the test frame, the base of the top chord did not rest squarely on the roller support at the south end of the joist. Similarly, for Joist No. 2, the north end did not sit squarely on the roller. Figure 2.19 shows the north support of Joist No. 2. This effect apparently was due to a permanent twist in the top chord. In each case, as load was applied to the joists during testing, the joist end straightened out and came into full contact with the roller bearing.

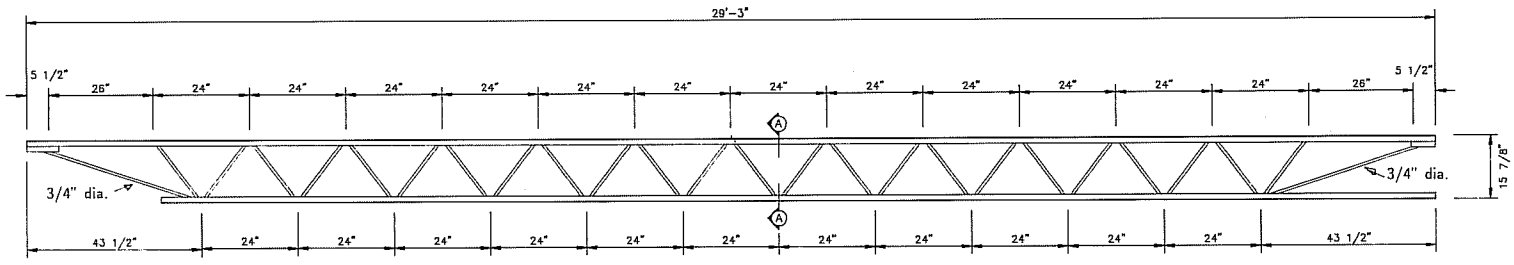

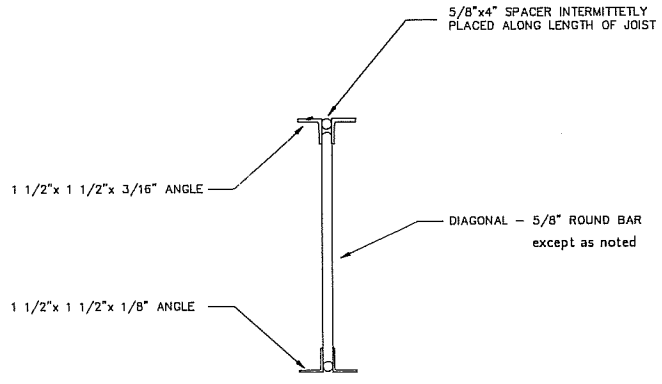

SECTION AA

NOTE: CONFIGURATION AND DIMENSIONS TO BE VERIFIED

JOIST CONFIGURATION AT SOUTH BAY	
HIGHLAND APPLIANCE DISTRIBUTION CENTER	
DATE: JULY 20, 1989	MEI NO. 89168
SCALE: NO SCALE	SHEET OF

MEI

Fig. 2.1 Nominal Joist Dimensions (from Morris Engineering Drawing)

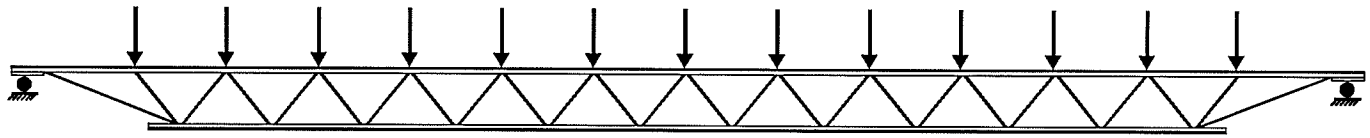

(a) Joist Nos. 1 and 2

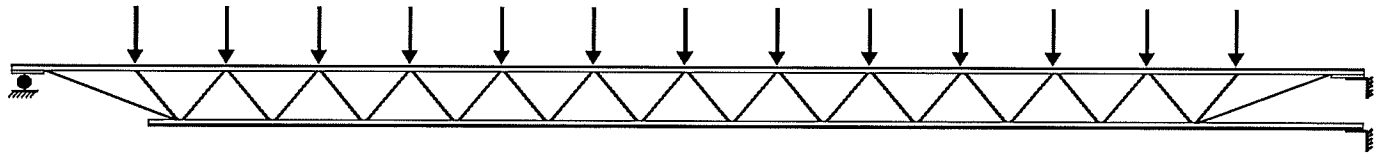

(b) Joist No. 3

= load (all loads nominally equal)

Fig. 2.2 Schematic Representation of Joist Tests

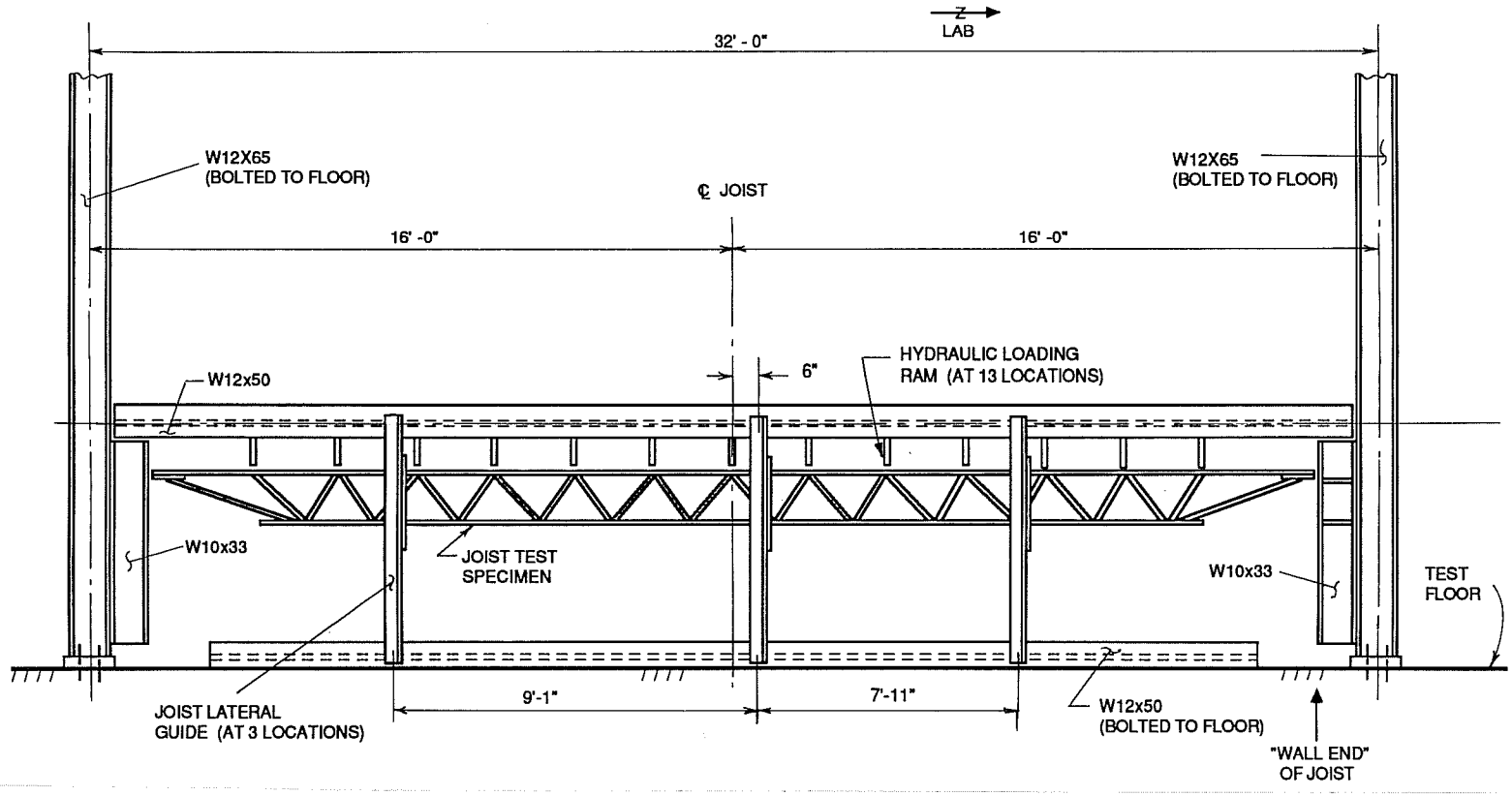

Fig. 2.3 Overall View of Test Setup

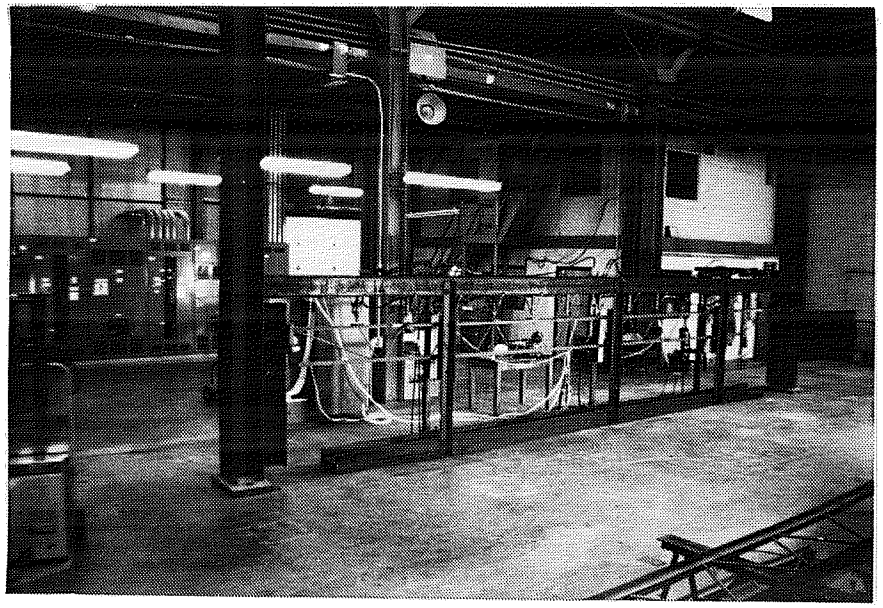

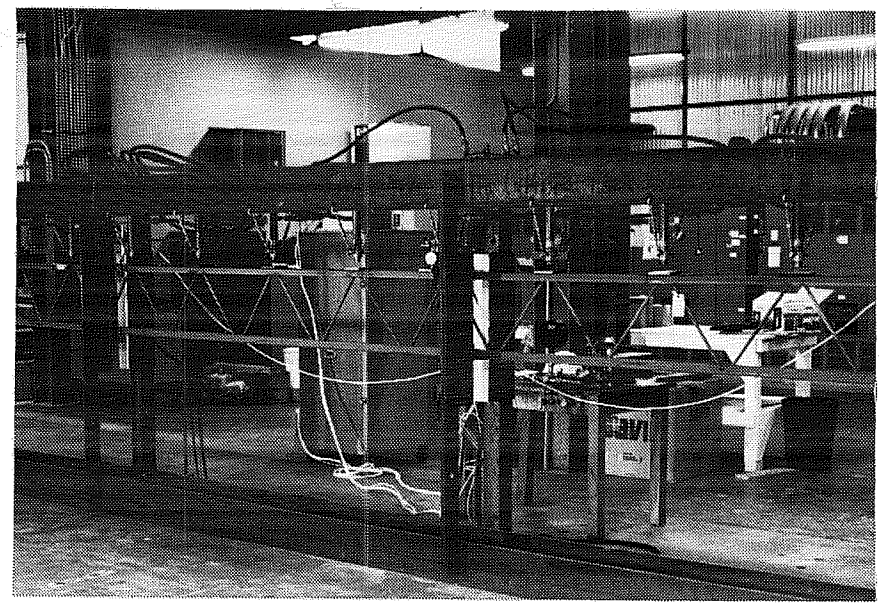

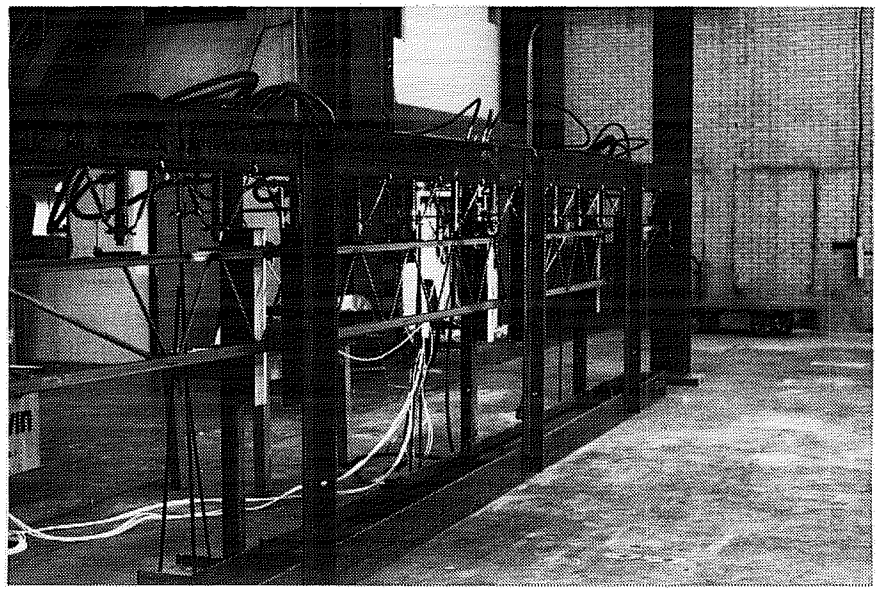

Fig. 2.4 Test Setup with Joist In Place

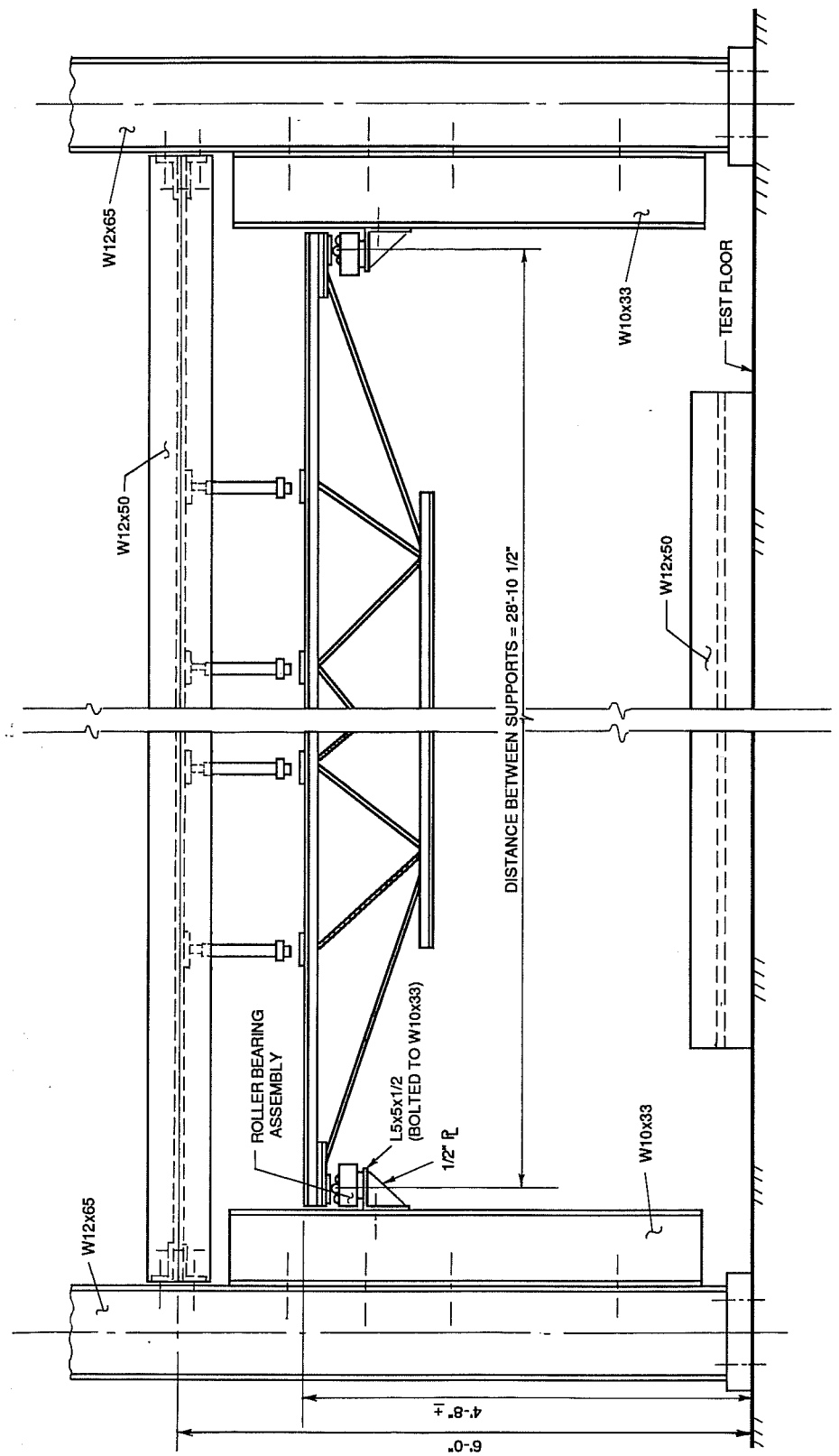

Fig. 2.5 End Support Details for Joist Nos. 1 and 2

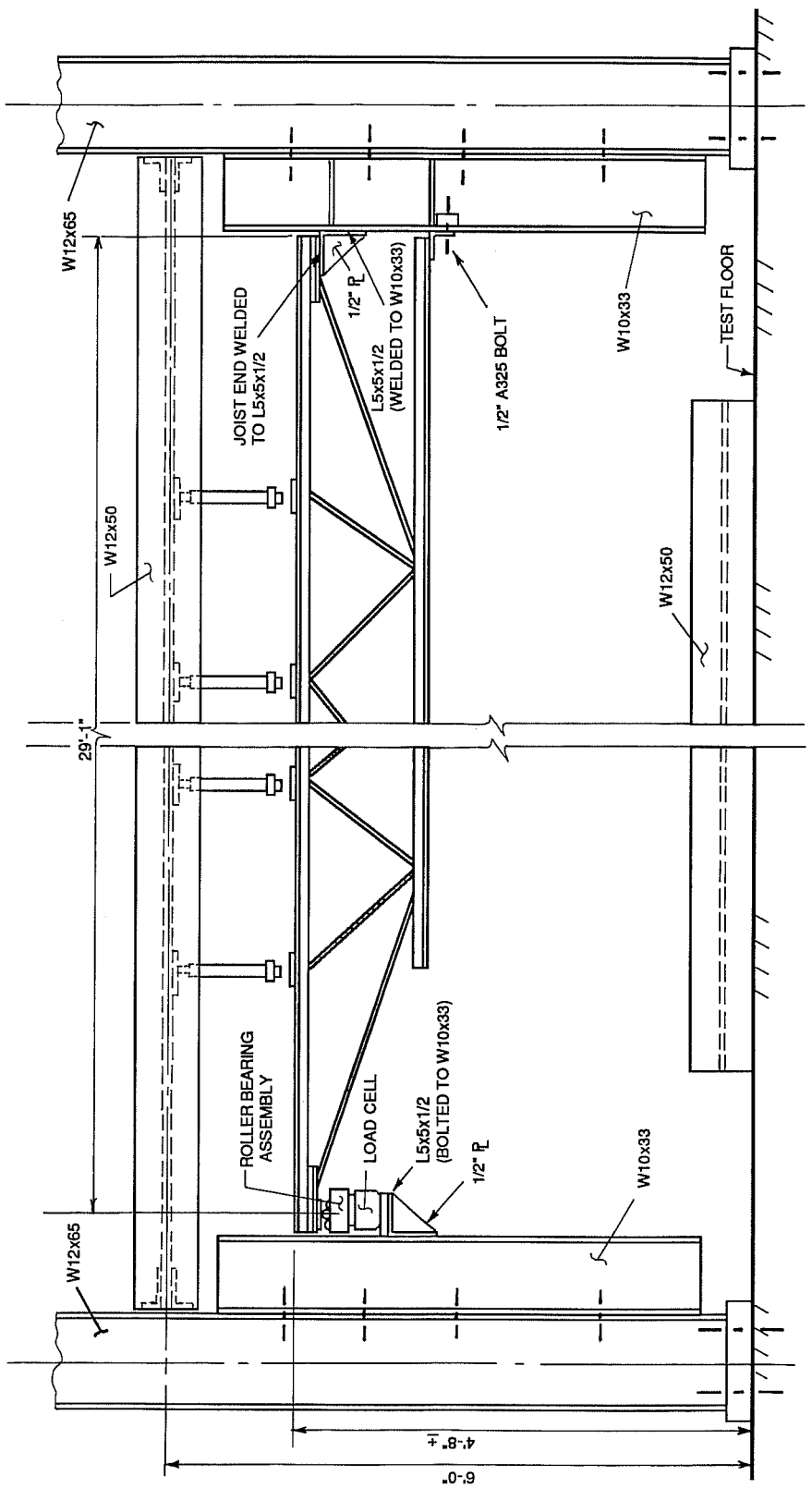

Fig. 2.6 End Support Details for Joist No. 3

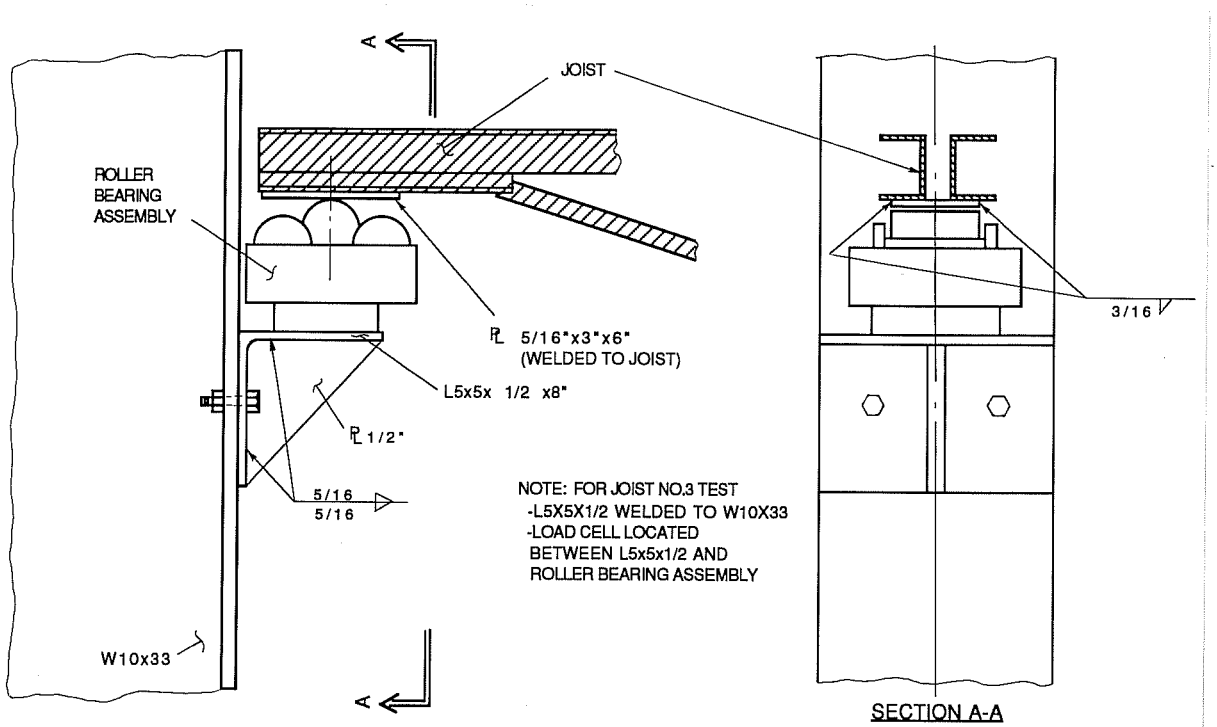

Fig. 2.7 Details at Roller Support

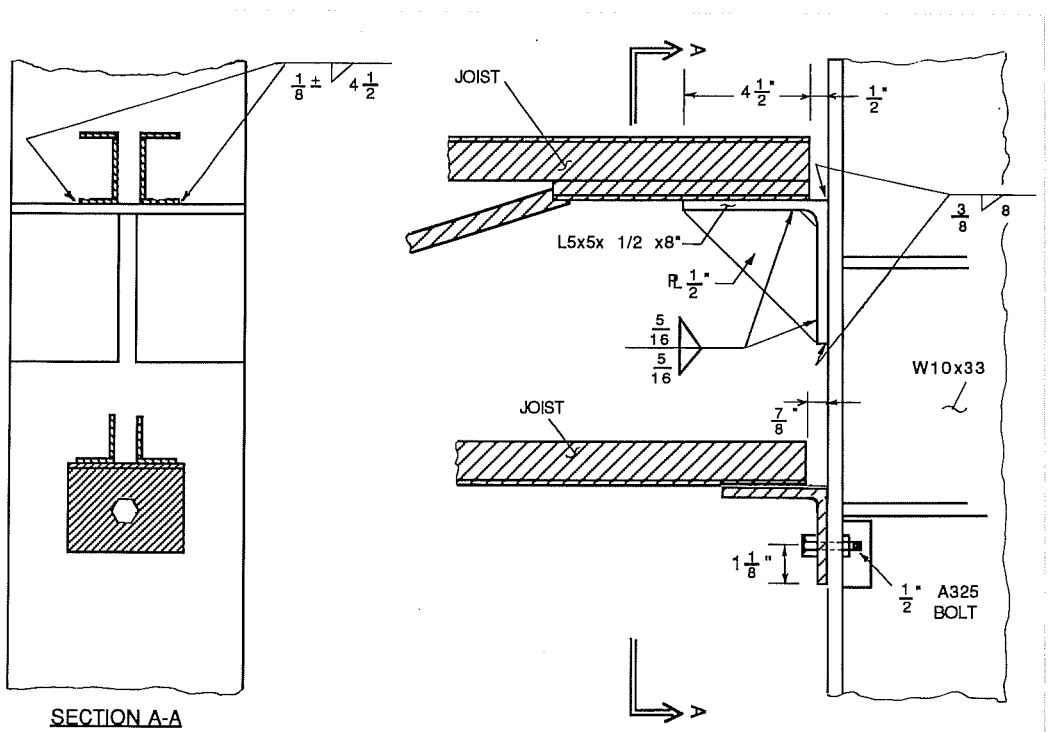

Fig. 2.8 Details at North End of Joist No. 3

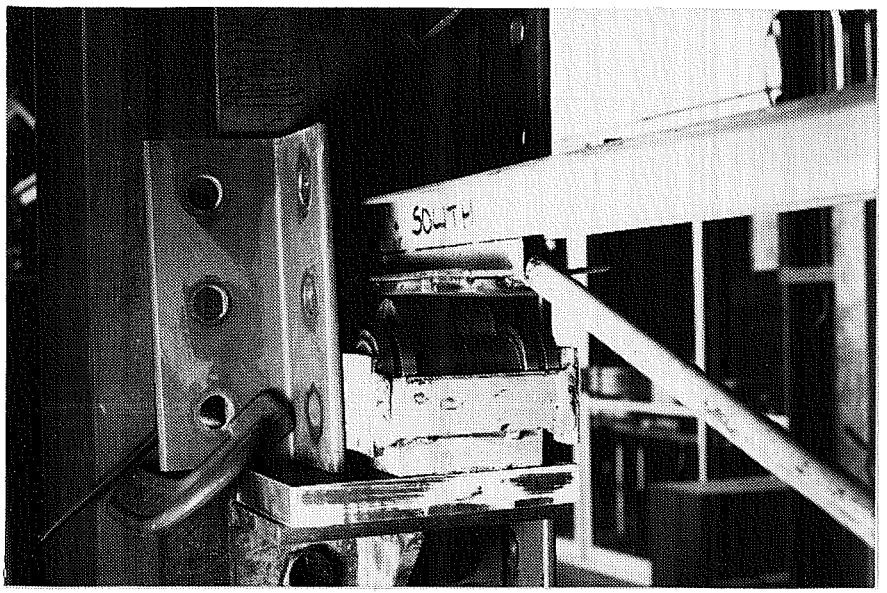

Fig. 2.9 Joist End Roller Support

Fig. 2.10 Connection at North End of Joist No. 3

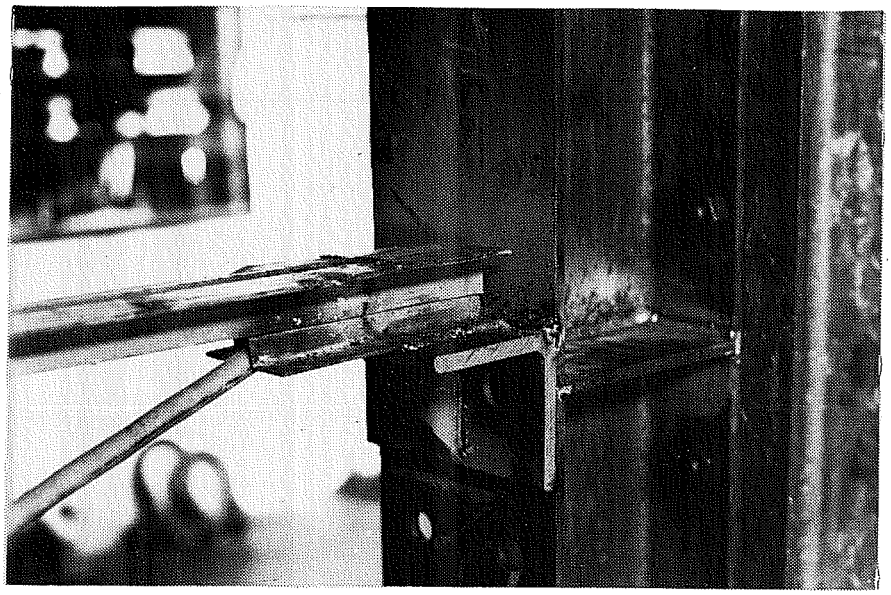

Fig. 2.10 Connection at North End of Joist No. 3 (cont.)

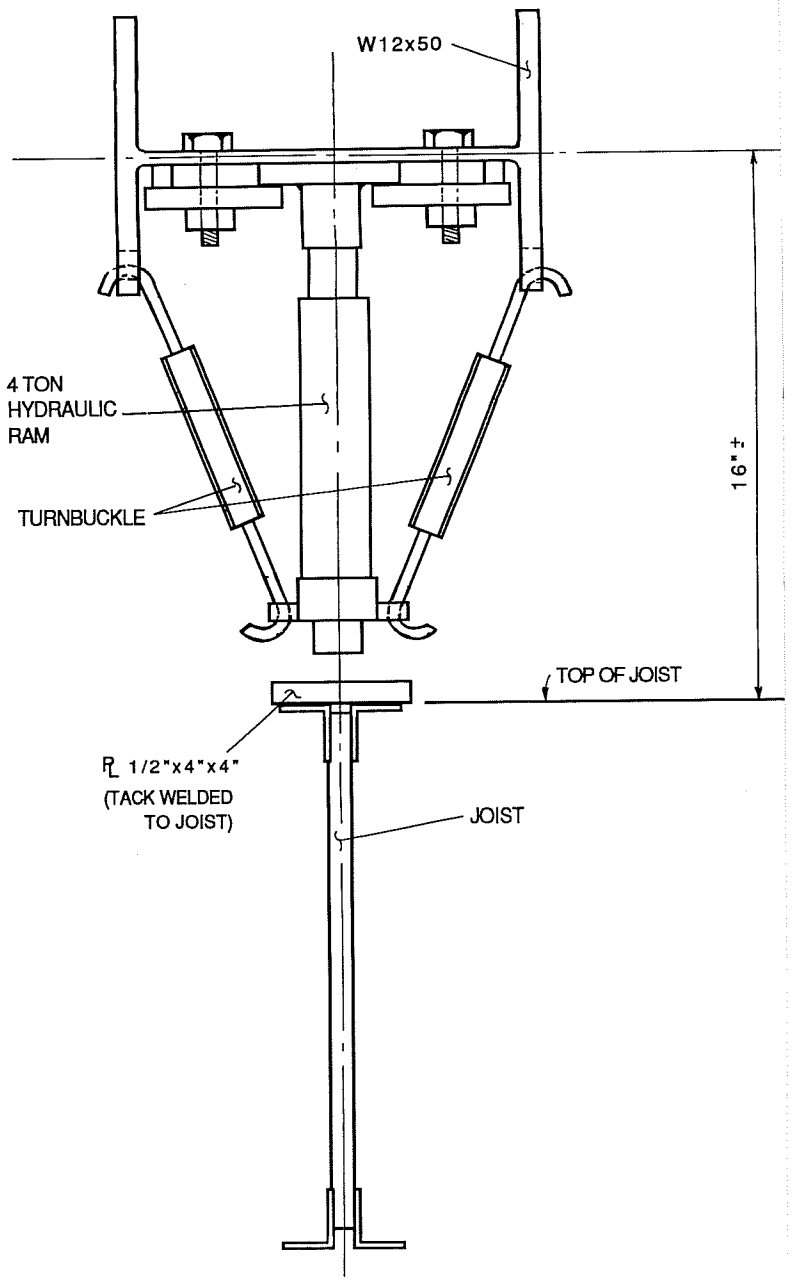

Fig. 2.11 Typical Detail at Hydraulic Loading Ram

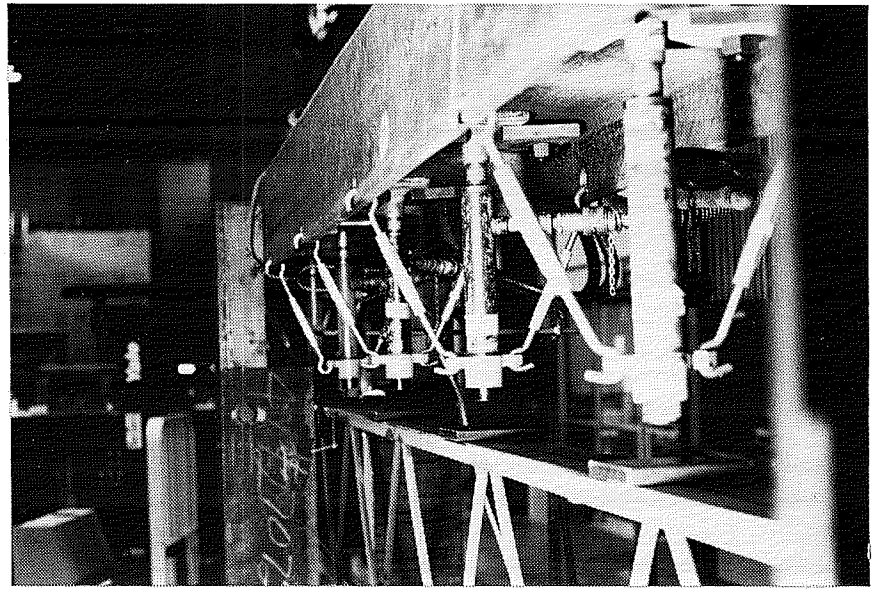

Fig. 2.12 Hydraulic Loading Rams

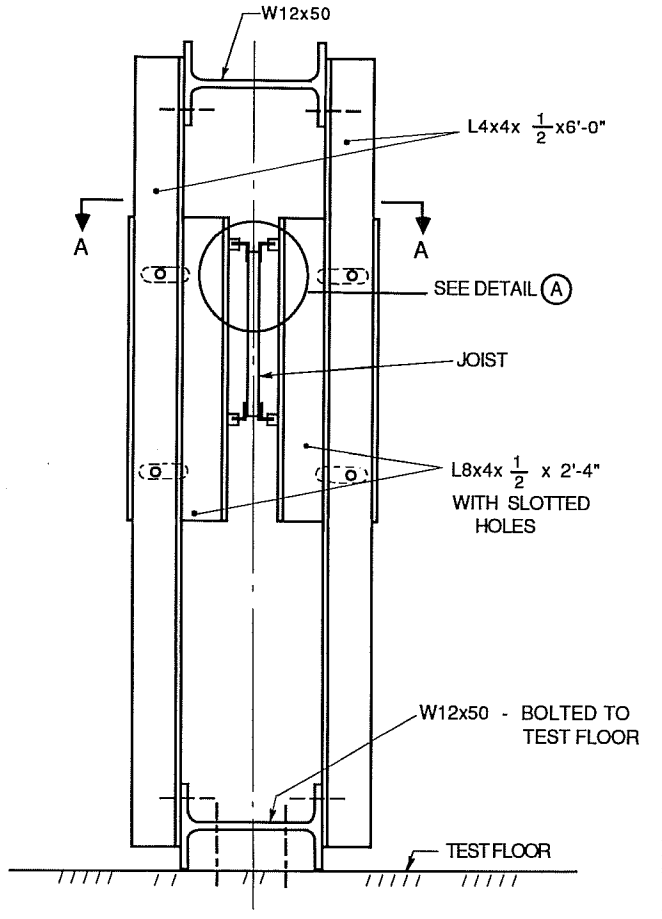

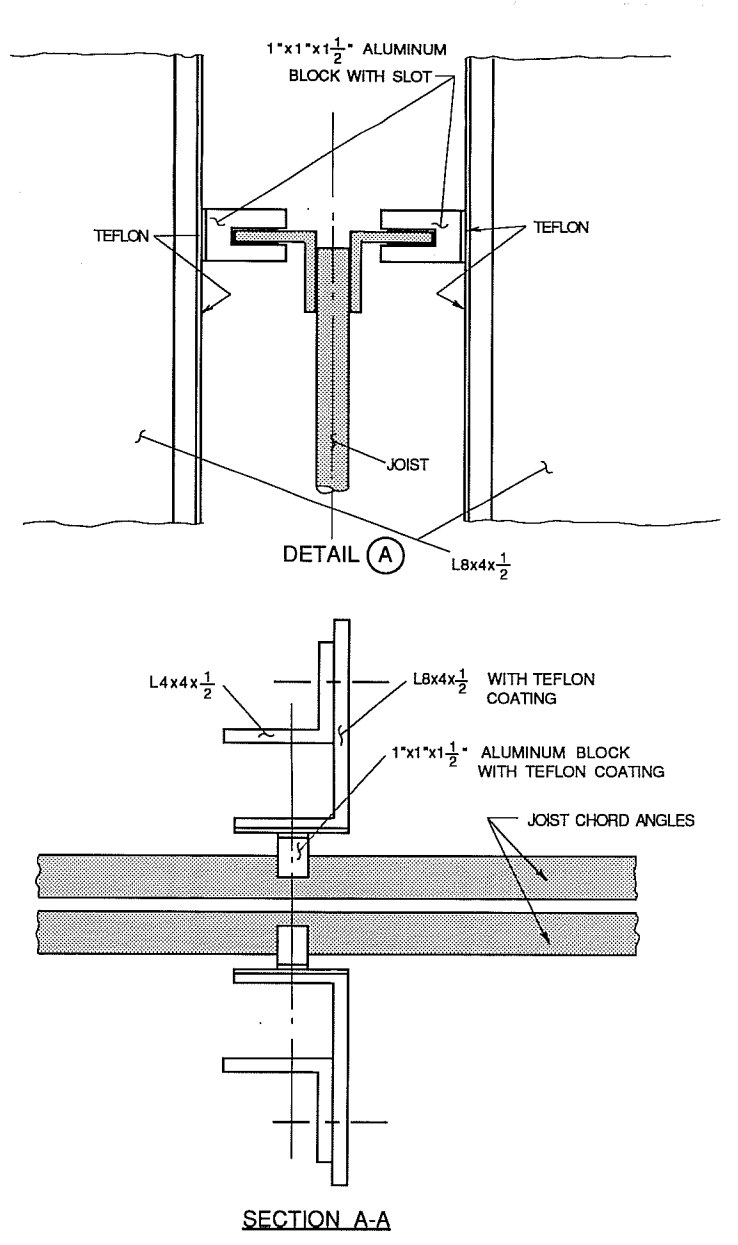

Fig. 2.13 Details at Joist Lateral Guide

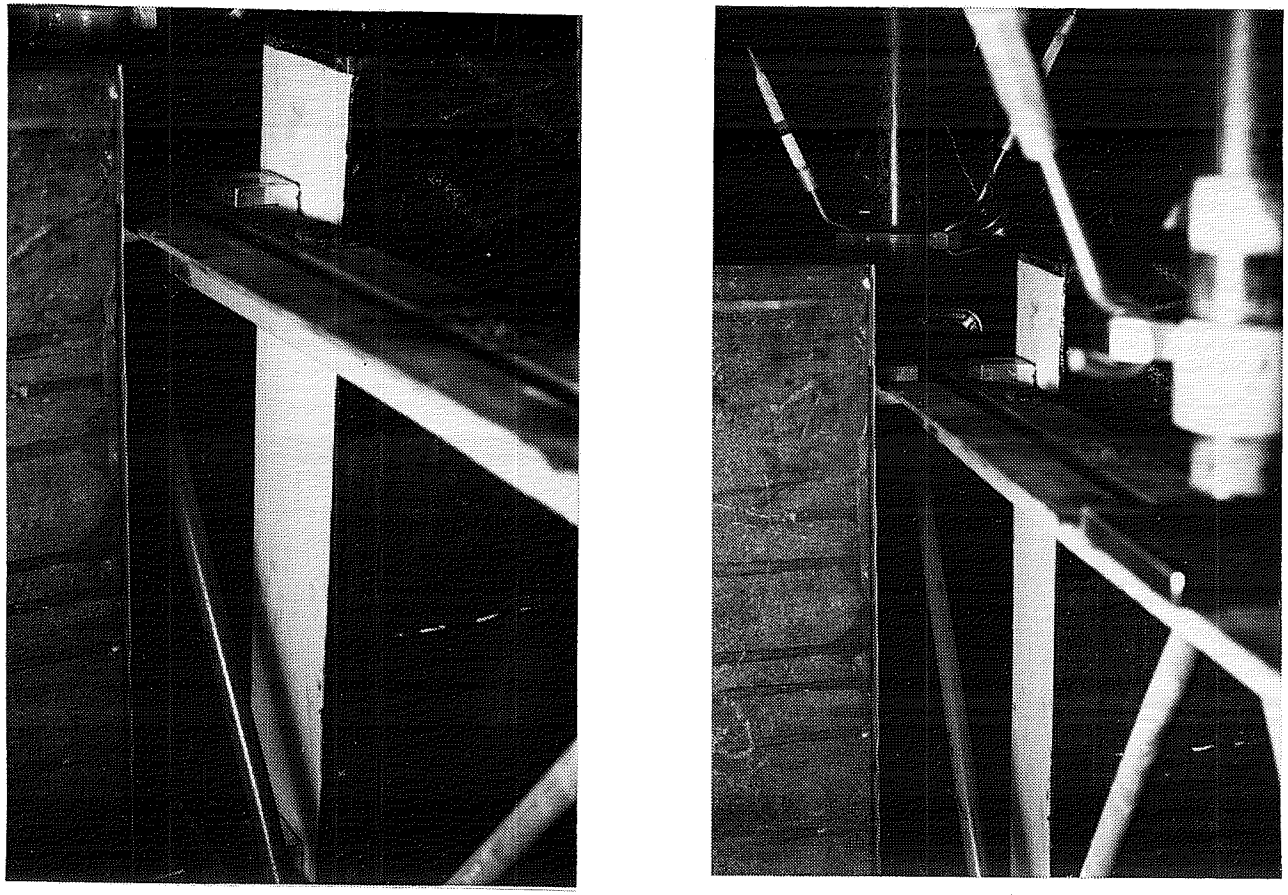

Fig. 2.14 Joist Lateral Guide

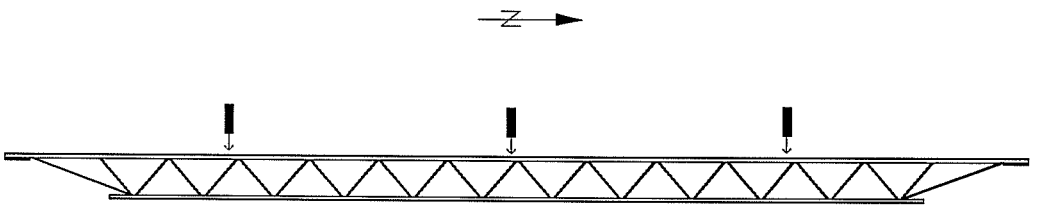

(a) Joist No. 1

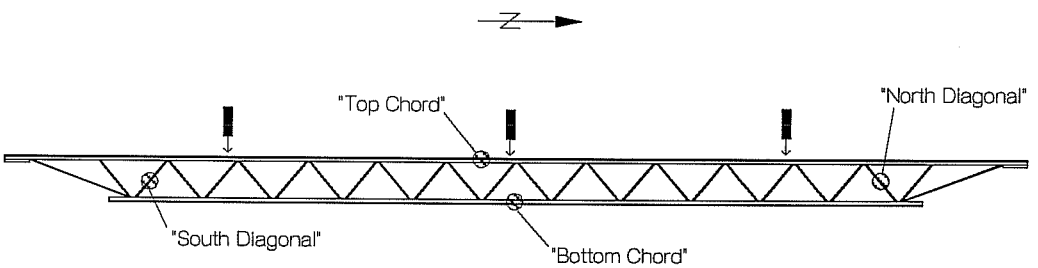

(b) Joist No. 2

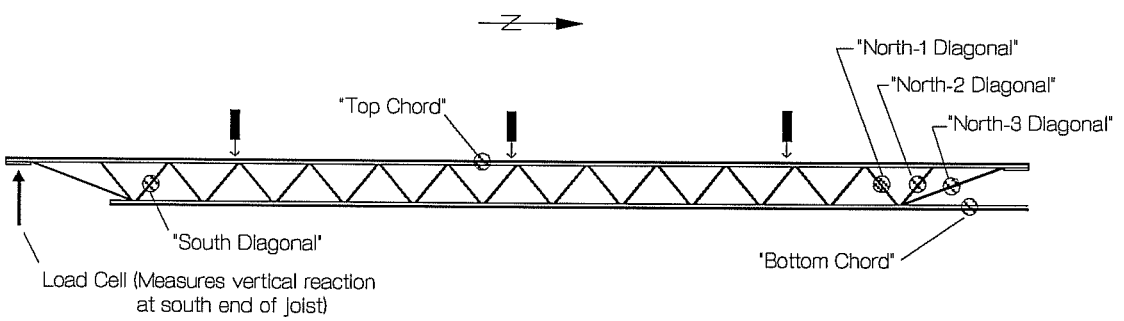

(c) Joist No. 3

= Vertical Displacement Transducer

= Strain Gaged Member

Note: Load monitoring instrumentation not shown

Fig. 2.15 Joist Instrumentation

(a) Strain Gage Locations on Diagonal Members
(4 gages at each location)

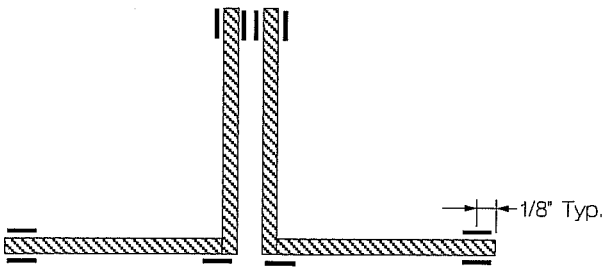

(b) Strain Gage Locations on Chord Members
(10 gages at each location)

Notes: - Gages located at approximately midlength of member
- All gages oriented longitudinally along member

Fig. 2.16 Layout of Strain Gages on Joist Diagonals and Chord Members

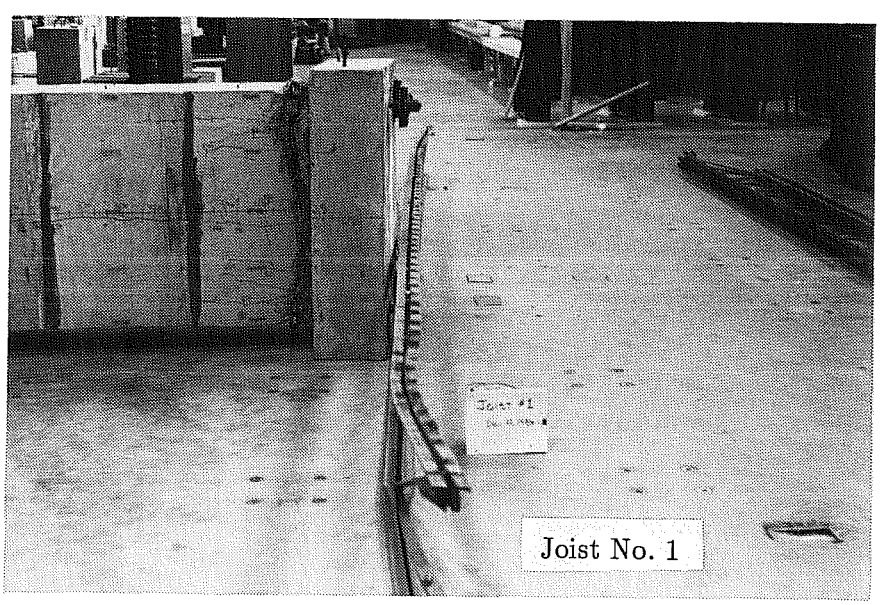

Fig. 2.17 Photographs of Joists as Received at Ferguson Lab

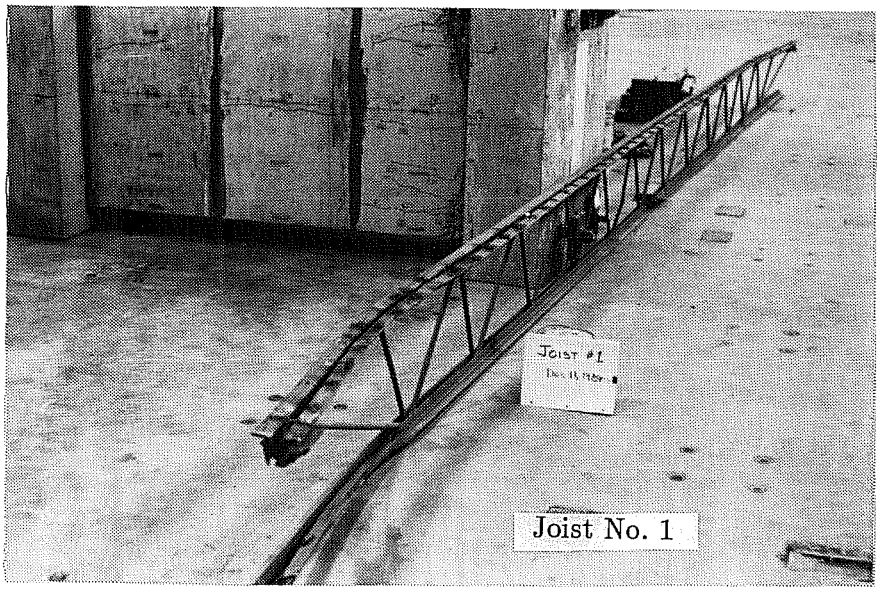

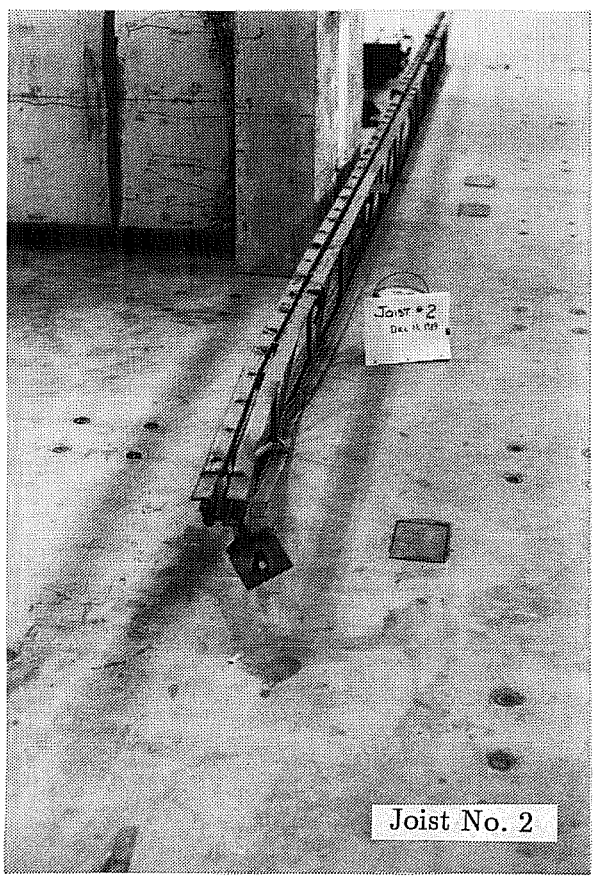

Fig. 2.17 Photographs of Joists as Received at Ferguson Lab (cont.)

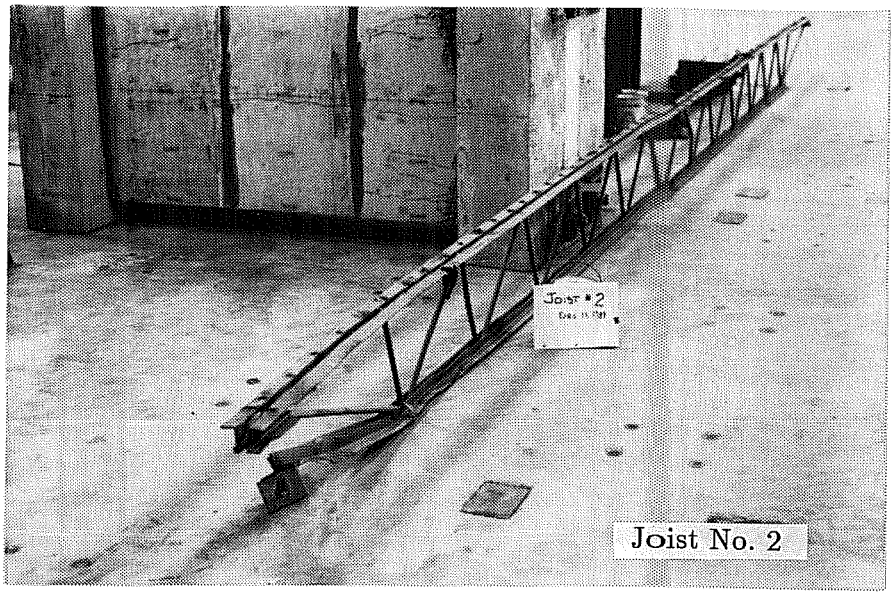

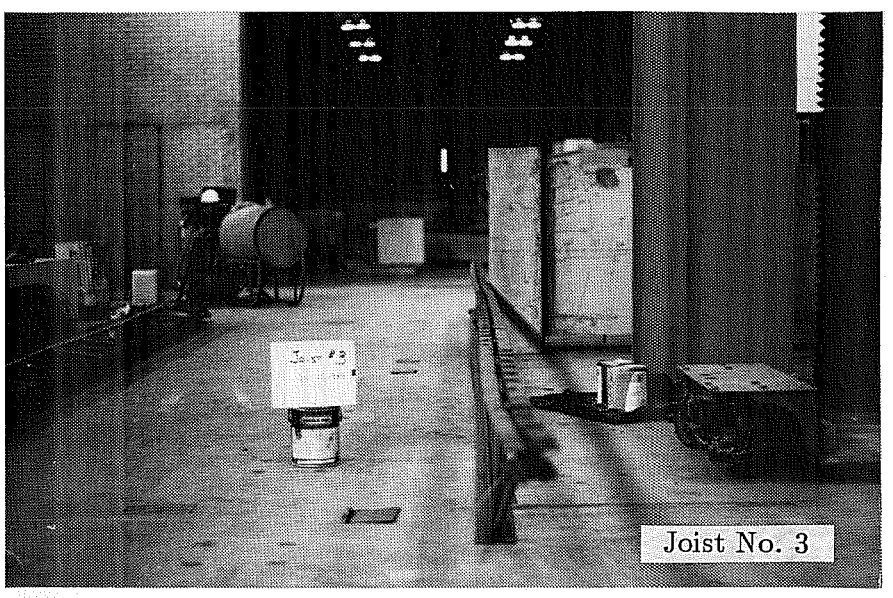

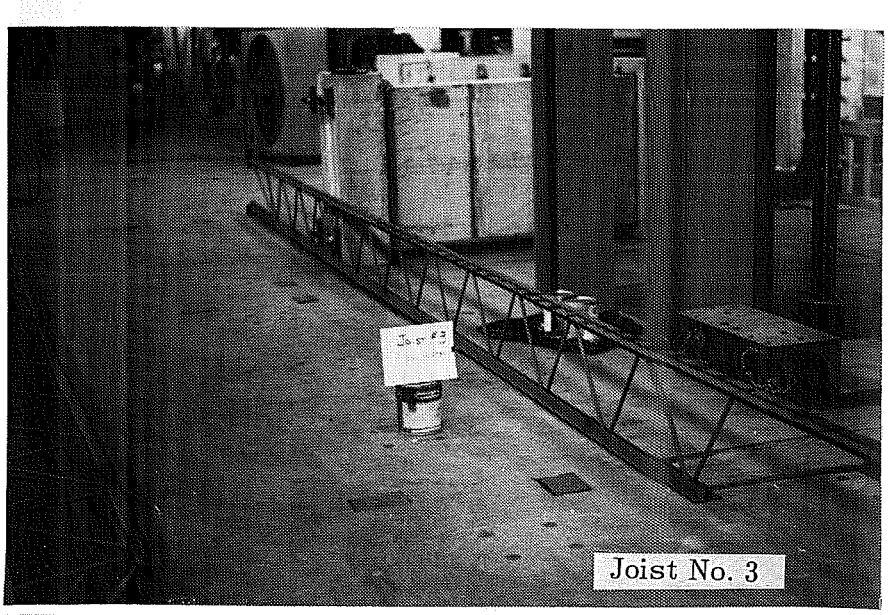

Fig. 2.17 Photographs of Joists as Received at Ferguson Lab (cont.)

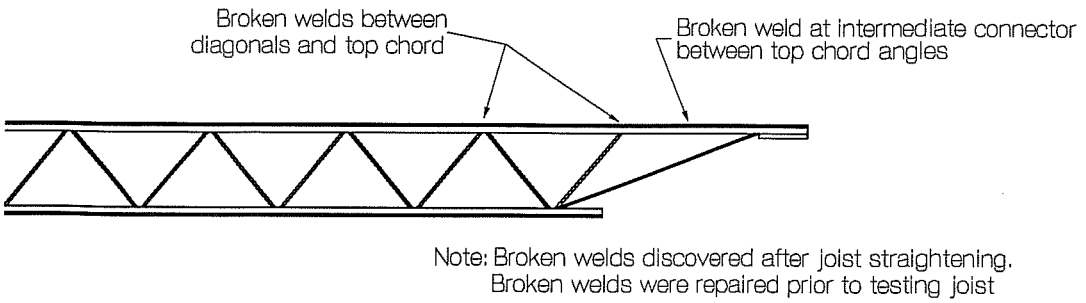

Fig. 2.18 Location of Broken Welds Found on Joist No. 1 After Straightening

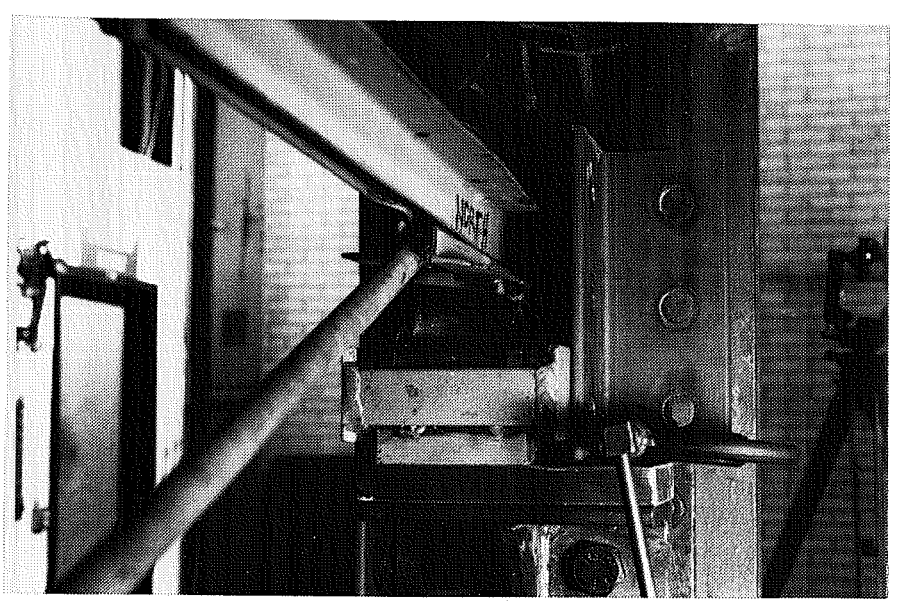

Fig. 2.19 North End of Joist No. 2 Prior to Testing

3. JOIST TESTS

General

This chapter describes the response of each joist during testing. Plots of load on the joist versus vertical displacement of the joist are provided, as well as a description and photographs of the failure mechanism for each joist. The load-displacement plots show the total downward vertical load on the joist. As described in Chapter 2, the total load was equally distributed among the 13 upper chord panel points (Fig. 2.2). For each joist, the downward displacement at each of the three displacement transducers are plotted. The displacements are labelled as "south", "center" and "north" according to the transducer locations shown in Fig. 2.15. Portions of the load-deflection plots corresponding to unloading of the joist after failure have been omitted for clarity. Strain gage data and lateral displacement data collected during each test are presented in Chapter 4.

Each of the three joist tests were conducted in a similar manner. Load was applied by means of a manual hydraulic pump. The load was increased in small intervals. At the end of each interval, loading was stopped (and held constant) while data readings (pressure, displacements, strain gages, etc.) were taken. Loading was continued until the peak strength of the joist was attained and a clearly observable failure mechanism developed. Joist Nos. 1, 2 and 3 were tested on January 4, 8 and 9, 1990, respectively.

Joist No. 1

The plot of load versus displacement for Joist No. 1 is shown in Fig. 3.1. The peak load held by this joist was 13,200 lbs., at which point the midspan deflection was measured at 3.01 inches. At the peak load, the first compression diagonal at the south end of the joist buckled. This was followed almost immediately by buckling of the next compression diagonal at the south end. The location of the buckled diagonals are indicated in Fig. 3.8. Photographs of the buckled diagonals are provided in Fig. 3.2. Both diagonals buckled primarily out of the plane of the joist. After all load was removed from the joist, the first compression diagonal at the south end had a residual out-of-straightness of approximately 1.75 inches at midlength. The residual out-of-straightness of the second compression diagonal that buckled was approximately 1 inch.

Prior to achieving the peak load, the load-displacement plot for Joist No. 1 (Fig. 3.1) shows some irregular areas where the displacements increased somewhat suddenly. These occurred at about 2000 lbs. and again at about 9000 lbs. It is believed that these increased displacements corresponded to slip in the joist end supports. The $5'' \times 5'' \times 1/2''$ support angles, bolted to the W10 x 33 support members likely slipped a small amount. During the test, sudden noises were heard from the supports, which indicated the likelihood of slip. For the remaining two joist tests, the connections were tightened, and no additional slipping occurred. The small slip of the end supports did not affect the strength of Joist No. 1, although the measured displacements were increased.

Joist No. 2

The plot of load versus displacement for Joist No. 2 is shown in Fig. 3.3. The peak load held by this joist was 11,100 lbs., at which point the midspan deflection was measured at 2.63 inches. At the peak load, the first compression diagonal at the north end of the joist buckled. Unlike Joist No. 1, no other members buckled. The location of the buckled diagonal is indicated in Fig. 3.8, and photographs of the failure are in Fig. 3.4. The diagonal buckled primarily out of the plane of the joist, with a similar buckled shape as occurred with Joist No. 1. As with Joist No. 1, the diagonal retained a permanent buckled shape after unloading of the joist at the end of the test.

Joist No. 3

The plot of load versus displacement for Joist No. 3 is shown in Fig. 3.5., and a plot of load versus the vertical reaction measured at the south end of the joist is in Fig. 3.6. The peak load held by this joist was 13,200 lbs., at which point the midspan deflection was measured at 2.37 inches. At the peak load, the first compression diagonal at the north end of the joist buckled. This diagonal buckled primarily in the plane of the joist.

After the first diagonal buckled, the load supported by the joist dropped to about 8700 lbs. At this point, loading of the joist was resumed. The load on the joist increased to approximately 10,500 lbs., at which point the second compression diagonal at the north end of the joist buckled. Again, the direction of buckling was primarily in the plane of the joist. After the second diagonal buckled, loading was again resumed. However, the hydraulic rams at the north end of the joist were fully extended shortly after the loading was resumed, and the test was terminated.

Figure 3.8 shows the location of the buckled diagonals in Joist No. 3. A photograph of the buckled diagonals is provided in Fig. 3.7. Both diagonals retained a permanent buckled shape after unloading of the joist at the end of the test.

In the initial loading of Joist No. 3, prior to buckling of the first diagonal, some interesting observations were made on the lower chord extension at the north end of the joist. When the load on the joist was at about 10,000 lbs., the lower chord extension was observed to be deflecting upwards. This upward deflection increased as the load on the joist approached its peak value of 13,200 lbs. This observation indicated the onset of buckling in the lower chord extension. Strain gage data for the lower chord extension (Chapter 4) also indicate instability of this member. No permanent deformation was visible in the lower chord extension after the joist was unloaded at the end of the test, indicating that the buckling in the lower chord extension was elastic.

Summary

The maximum load sustained by each joist, and the corresponding midspan deflection are summarized in Table 3.1

TABLE 3.1
Summary of Maximum Joist Loads

Joist	Maximum Load	Midspan Deflection at Maximum Load
1	13,200 lbs.	3.01 in.
2	11,100 lbs.	2.63 in.
3	13,200 lbs.	2.37 in.

The maximum midspan deflection measured for Joist No. 3 was significantly lower than for the other two joists, due to the stiffening effect of the lower chord extension.

Each joist failed by buckling of compression diagonals near the joist end. In Joist No. 1, the first two compression diagonals at the south end buckled out of the plane of the joist. In Joist No. 2, the first compression diagonal at the north end buckled out of the plane of the joist. In Joist No. 3, the first compression diagonal at the north end buckled in the plane of the joist. Upon continued loading, the second compression diagonal at the north end also buckled in the plane of the joist. There was also evidence of buckling of the lower chord extension in the plane of the joist for Joist No. 3.

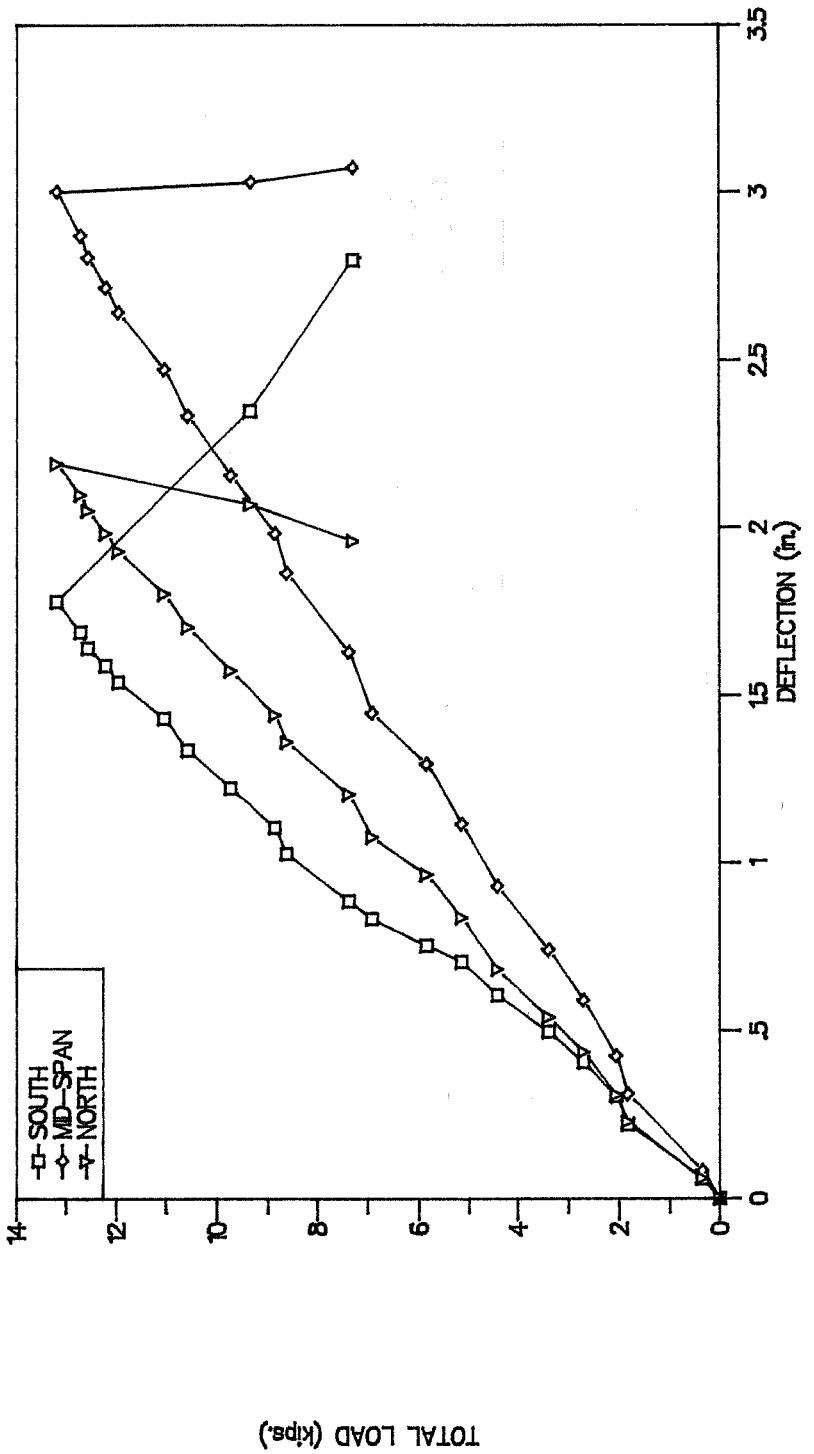

Fig. 3.1 Joist No. 1 – Load vs. Displacement

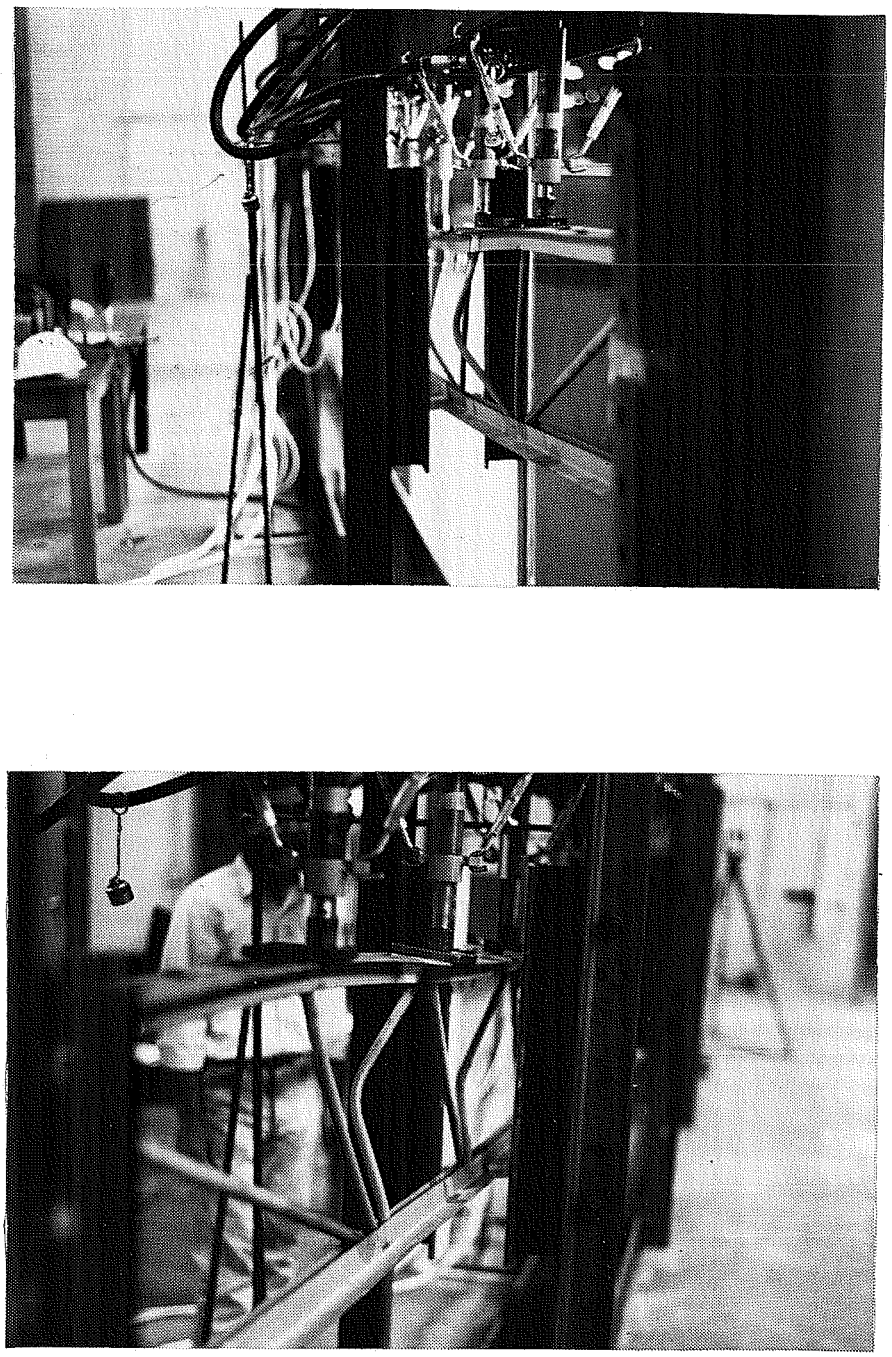

Fig. 3.2 Joist No. 1 – After Testing

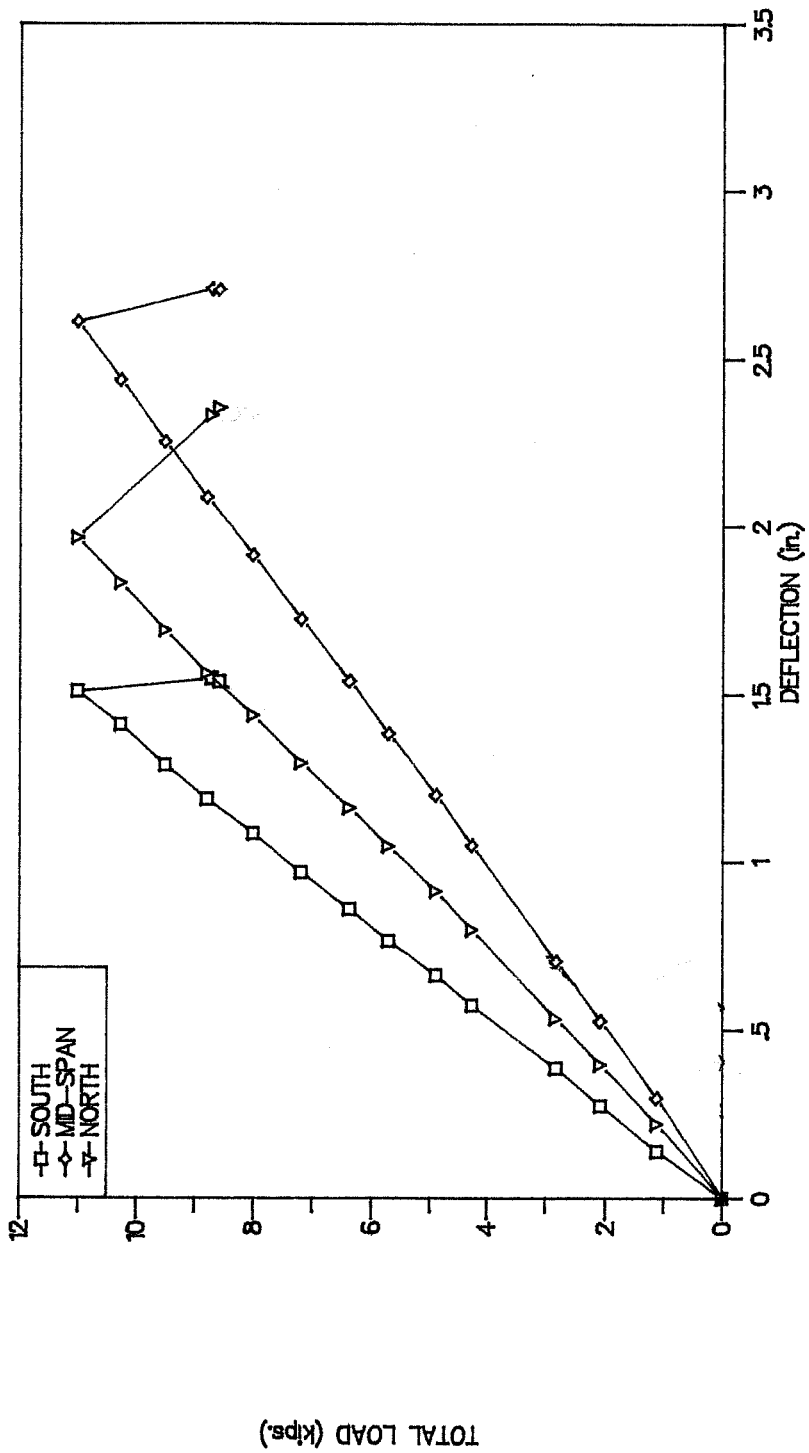

Fig. 3.3 Joist No. 2 – Load vs. Displacement

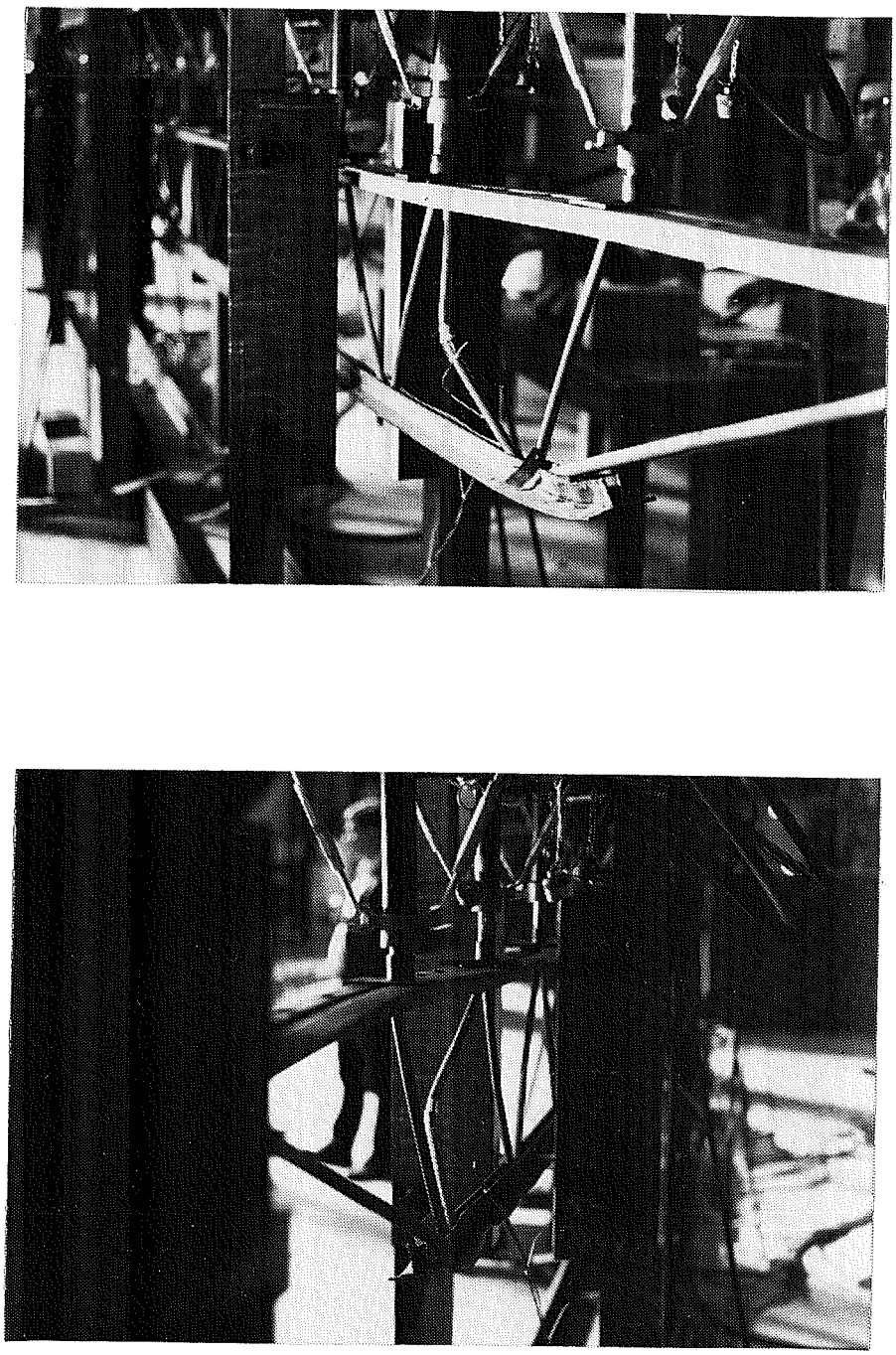

Fig. 3.4 Joist No. 2 – After Testing

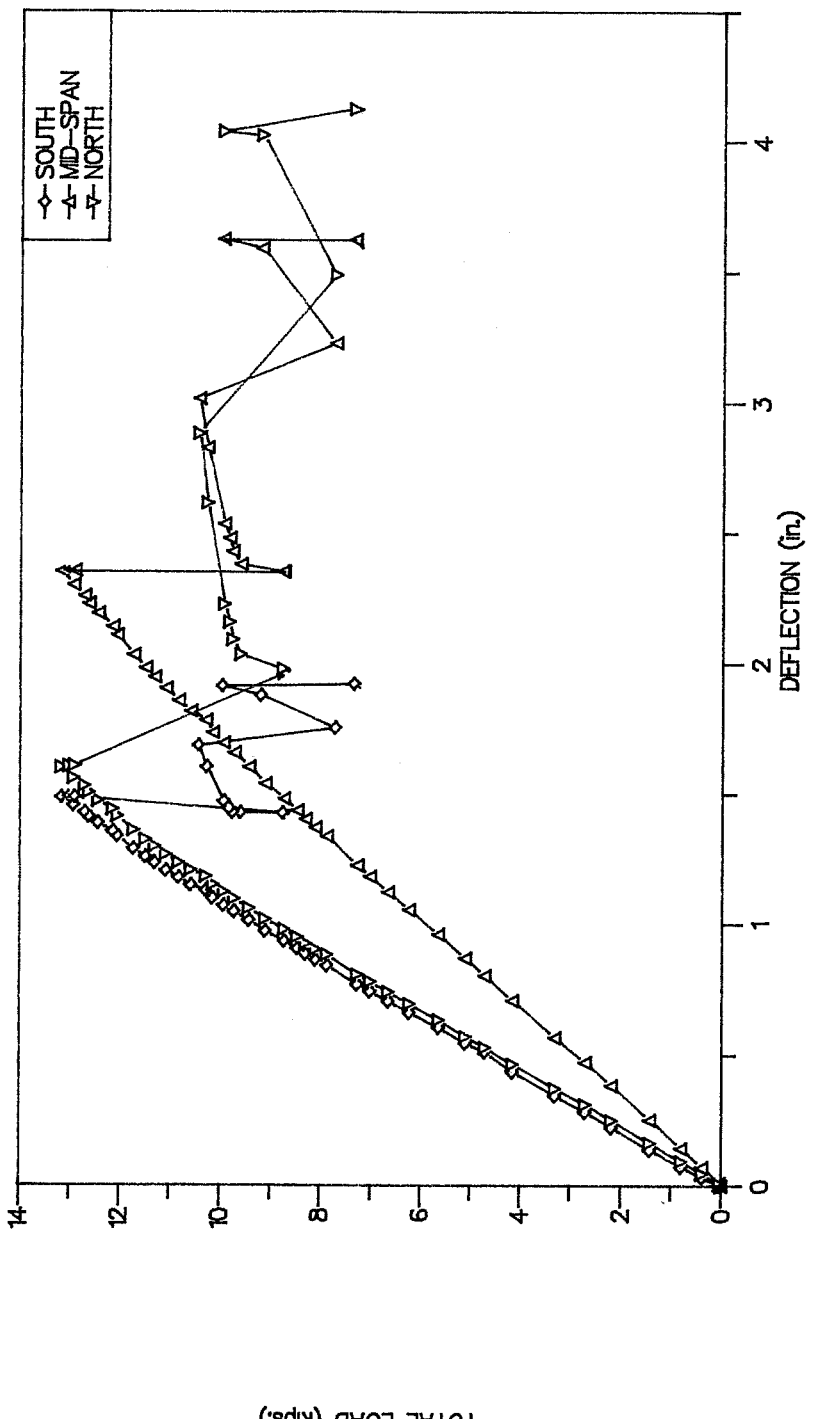

Fig. 3.5 Joist No. 3 –Load vs. Displacement

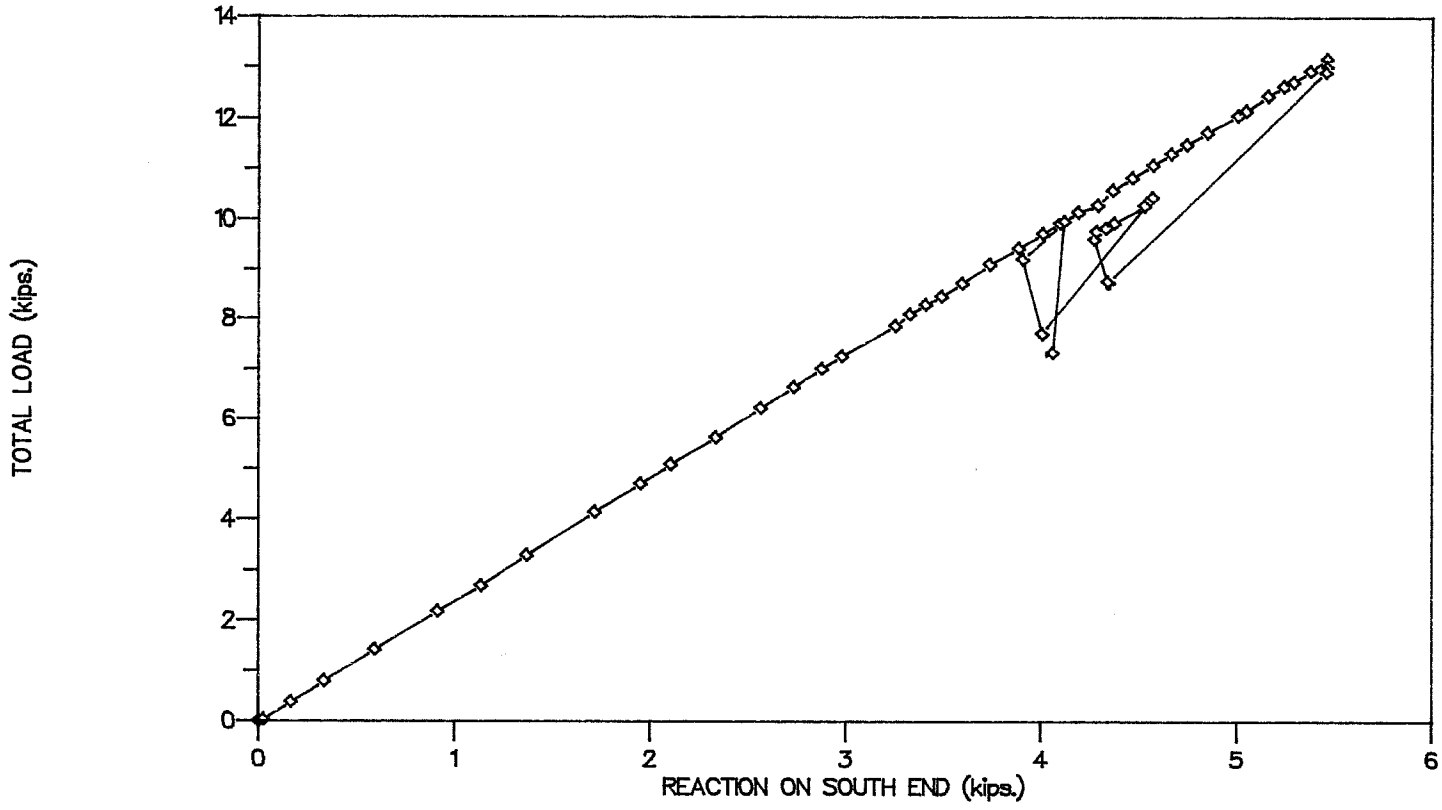

Fig. 3.6 Joist No. 3 – Load vs. Reaction at South End of Joist

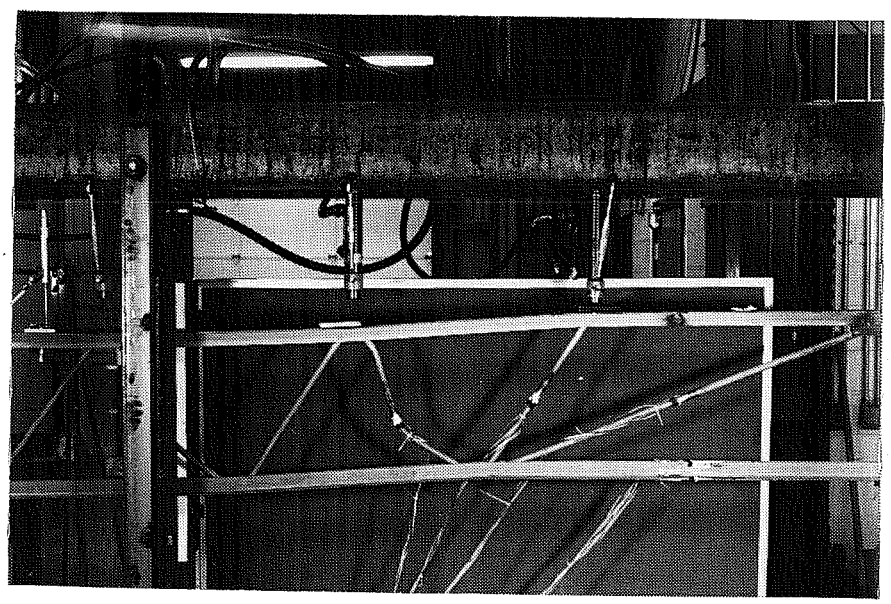

Fig. 3.7 Joist No. 3 – After Testing

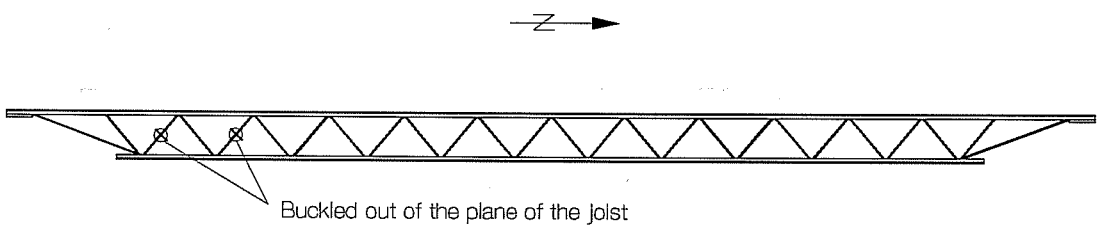

(a) Joist No. 1

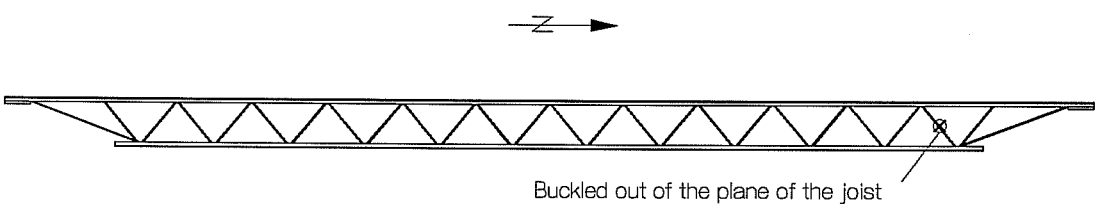

(b) Joist No. 2

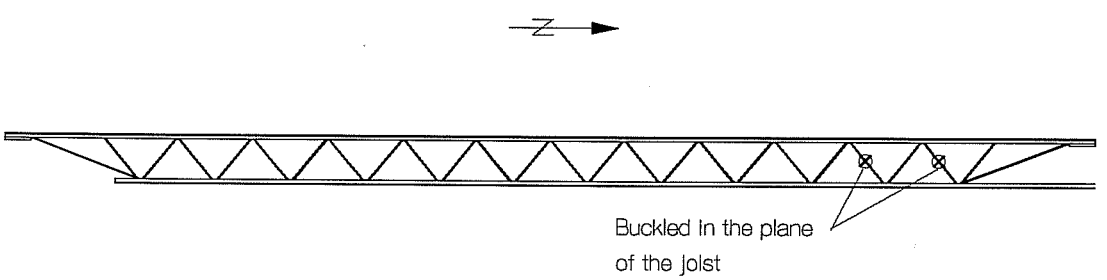

(c) Joist No. 3

Fig. 3.8 Location of Buckled Diagonals

4. ADDITIONAL TEST DATA

Joist Out-of-Plane Displacements

As noted in Chapter 2, measurements of lateral displacement of the joists were taken during each test. Prior to each test, a transit was set up near the joist, and a line of sight was established approximately parallel to the joist. The line of sight was chosen so that the distance from the line of sight to the joist was approximately equal for the two ends of the joist. The distance from the line of sight to points on the joist were determined by holding a scale to the joist, and then reading the scale with the transit. These measurements were taken to check for out-of-plane movement of the top chord in order to assess the effectiveness of the lateral support system. The measurements also provided an indication of the initial crookedness of the joists prior to testing.

The locations at which lateral displacement readings were taken on each joist are shown in Fig. 4.1. For each joist, readings were taken along the top chord at the joist ends and midway between the panel points. Two points were also monitored along the bottom chord of Joist No. 3. For each joist, a full set of readings were taken along the unloaded joist at the start of each test. Selected points were then read at several times throughout the test. A full set of readings were also taken along the unloaded joist at the end of the test.

The lateral displacement readings for each joist are presented in Tables 4.1 to 4.3. At each location along the joist, the absolute reading is provided, as well as the change in reading from the initial unloaded state. Some selected results are shown graphically in Fig. 4.1a. The initial shape from a straight line through the two end supports is shown for each joist. Each joist had an initial lateral displacement of the top chord of at least 1/2 inch over most of the length. The data suggest that each joist had a kink near the first panel point at each end. This initial deformation pattern is also visible in the photographs in Fig. 2.17.

Because the top chord was laterally braced, these initial deformations had little effect on the joist behavior. This is demonstrated by the lateral displacements measured prior to buckling of the end diagonal and also after buckling. For Joist No. 1, the lateral displacements of the top chord at 12,000 lb. (maximum = 13,200 lb.) show only slight deviations from the initial shape. There is a significant change in lateral displacement only after the failure load was reached. In Joist No. 2, the lateral displacement did not even change significantly after buckling. The same observation can be applied to Joist No. 3; the data are not shown in Fig. 4.1a for clarity.

Strain Gage Data

Data Reduction

As noted in Chapter 2, selected diagonal and chord members were instrumented with electrical resistance strain gages on Joist Nos. 2 and 3. The location of the gaged members are indicated in Fig. 2.15, and typical gage layouts are shown in Fig. 2.16.

The purpose of the strain gages was to provide an estimate of the axial force in the gaged members throughout the test. The joist members, in general, were subject to both axial force and bending moments. Consequently, the strain at any one location of the member represents a combination of axial strain and bending strain. The gage layouts were chosen to permit computation of axial strain in the member.

On the circular diagonals, four diametrically opposite gages were provided, as indicated in Fig. 2.16. Due the symmetry of the cross-section, the bending neutral axis must pass through the center of the section, and the axial strain can be computed by simply taking the average of the four strain gage readings. The average cancels out the bending strains. Gages on diagonal members that buckled became inoperative after buckling. Therefore, strain gage data is reported for these members only up to the point of buckling.

For the double angle chord members, ten gages were provided (Fig. 2.16). The behavior of these members is considerably more complex than that of the diagonals. The location of the bending neutral axis is uncertain in the double angle members, because the angles can bend as a composite unit, but can also bend individually. Consequently, the axial strain in the double angle members was computed using a technique that did not require knowledge of the neutral axis location. The method used to compute axial strain is outlined in Fig. 4.2, and is based on the assumption that plane sections remain plane for each individual angle of the double angle member. Since no local buckling was observed in the angles during the tests, this appears to be a valid assumption.

It should be noted that the strain gage readings, and the resulting computed axial strains, represent changes in strain with respect to the unloaded condition at the start of the test. The readings do not include residual strains that may have been in the members at the start of the test. Residual strains may have been present due to several causes, including initial forming of the steel members, initial fabrication of the joists, and any bending of the joists resulting from the roof collapse and subsequent straightening operations.

After the axial strain was computed in the members, the axial stress was estimated by multiplying strain by the modulus of elasticity of steel (30,000 ksi). This is based on the assumption that the material was within the elastic range at the location of the strain gages. Tensile coupon data for the three test joists were not available, and so the actual yield stress of the material is unknown. However, tensile coupon data provided by Morris Engineering for other joists from the warehouse roof indicated yield points of at least 57 ksi for both diagonals and chord members. None of the elastically computed stresses at strain gage locations exceeded 57 ksi prior to achieving the peak load on the joist. Thus, if it is assumed that the available coupon data is representative of the test joists, none of the measured strains exceeded the yield strain of the material prior to joist failure. Nonetheless, if significant residual strains were present in the members before testing, localized yielding of the members may still have occurred, even though the measured strains were below the yield strain. Thus, the computed stresses, based on assumed elastic behavior, must be interpreted with caution.

After axial stress in the members was estimated, the axial force was computed by multiplying the stress by the cross-sectional area of the member. The area was estimated from cross-sectional dimensions measured at the strain gage locations.

Axial Strains and Forces

Results of the strain and force computations are presented in Figs. 4.3 to 4.10. Member designations are keyed to those given in Fig. 2.15. For each gaged member, two plots are provided: axial strain versus total load on the joist, and axial force versus total load on the joist. Some portions of the plots corresponding to unloading of the joists after failure are omitted for clarity.

As discussed above, these plots must be interpreted with caution. This is particularly true for the axial force plots, which are based on assumed elastic response (to convert strain to stress) and an estimated cross-sectional area (to convert stress to force). A linear relationship between joist load and member force indicates elastic member response. Most of the plots in Figs. 4.3 to 4.10 are in fact linear, indicating the assumption of elastic behavior is reasonable. Nonlinear response can be seen in the north diagonal of Joist No. 2 (Fig. 4.3) just prior to buckling, indicating the possibility of some yielding in this member just prior to buckling.

Figs. 4.9 and 4.10 show some interesting results for the bottom chord extension in Joist No. 3. These plots indicate that the force in the bottom chord extension did not increase in proportion to the load on the joist. These data indicate buckling of the bottom chord extension, consistent with visual observations made during the test (see Chapter 3). The bottom chord extension appears to have buckled elastically, since no residual deformation was visible in the member at the end of the test. The nonlinear relationship between joist load and the force in the bottom chord extension in Figs. 4.9 and 4.10 is therefore the result of elastic buckling of the member and not due to yielding of the member. The elastic buckling of the bottom chord extension explains the somewhat nonlinear load – deflection plots for Joist No. 3 (Fig. 3.5).

TABLE 4.1

JOIST NO. 1

Transit Reading for Lateral Displacements

(All Readings in mm)

Total Load on Joist (lbs.)	*Joist Location*													
	1	2	3	4	5	6	7	8	9	10	11	12	13	14
0	51	61	64	66	67	66	64	64	65	66	68	64	47	50
2700	-	61 (0)	-	-	67 (0)	-	-	-	66 (1)	-	-	-	46 (-1)	-
5900	-	62 (1)	-	-	67 (0)	-	-	-	65 (0)	-	-	-	45 (-2)	-
8900	-	63 (2)	-	-	67 (0)	-	-	-	66 (1)	-	-	-	43 (-4)	-
12000	-	63 (2)	64 (0)	66 (0)	67 (0)	65 (-1)	64 (0)	63 (-1)	66 (1)	69 (3)	71 (3)	63 (-1)	41 (-6)	-
7300*	53 (2)	65 (4)	66 (2)	67 (1)	67 (0)	66 (0)	66 (2)	69 (5)	76 (11)	81 (15)	79 (11)	63 (-1)	38 (-9)	50 (0)
0*	53 (2)	63 (2)	65 (1)	67 (1)	68 (1)	68 (2)	67 (3)	67 (3)	69 (4)	72 (6)	73 (5)	65 (1)	47 (0)	50 (0)

Notes:
1. See Fig. 4.1 for location of readings
2. - indicates no reading taken
3. Number in parenthesis ( ) indicates change in reading from initial (zero load) reading
4. Positive number in parenthesis indicates eastward displacement
5. Negative number in parenthesis indicates westward displacement
6. * indicates readings were taken after the peak load was achieved (i. e. after failure)

TABLE 4.2

JOIST NO. 2

Transit Reading for Lateral Displacements

(All Readings in mm)

Total Load on Joist (lbs.)	*Joist Location*													
	1	2	3	4	5	6	7	8	9	10	11	12	13	14
0	59	83	82	77	75	75	76	75	73	72	73	75	75	62
2900	-	82 (-1)	-	-	74 (-1)	-	-	-	73 (0)	-	-	-	76 (1)	-
5600	-	82 (-1)	-	-	75 (0)	-	-	-	72 (-1)	-	-	-	76 (1)	-
8900	-	83 (0)	-	-	75 (0)	-	-	-	72 (-1)	-	-	-	77 (2)	-
8800*	52 (-7)	87 (4)	82 (0)	76 (-1)	74 (-1)	74 (-1)	76 (0)	74 (-1)	71 (-2)	69 (-3)	71 (-2)	75 (0)	78 (3)	65 (3)
0*	59 (0)	82 (-1)	81 (-1)	77 (0)	75 (0)	75 (0)	75 (-1)	74 (-1)	72 (-1)	71 (-1)	73 (0)	75 (0)	75 (0)	62 (0)

Notes:
1. See Fig. 4.1 for location of readings
2. - indicates no reading taken
3. Number in parenthesis ( ) indicates change in reading from initial (zero load) reading
4. Positive number in parenthesis indicates eastward displacement
5. Negative number in parenthesis indicates westward displacement
6. * indicates readings were taken after the peak load was achieved (i. e. after failure)

TABLE 4.3

JOIST NO. 3

Transit Reading for Lateral Displacements

(All Readings in mm)

Total Load on Joist (lbs.)	*Joist Location*																
	1	2	3	4	5	6	7	8	9	10	11	12	13	14	15	16	17
0	43	15	31	20	16	15	11	8	10	14	18	22	23	22	21	18	41
2700	-	17 (2)	31 (0)	19 (-1)	16 (0)	16 (1)	-	10 (2)	-	-	-	22 (0)	-	-	-	19 (1)	-
5700	-	18 (3)	31 (0)	19 (-1)	16 (0)	17 (2)	-	9 (1)	-	-	-	22 (0)	-	-	-	18 (0)	-
8800	-	19 (4)	30 (-1)	19 (-1)	16 (0)	17 (2)	-	9 (1)	-	-	-	22 (0)	-	-	-	18 (0)	-
12100	-	19 (4)	28 (-3)	16 (-4)	13 (-3)	17 (2)	-	6 (-2)	-	-	-	19 (-3)	-	-	-	13 (-5)	-
10000*	-	17 (2)	27 (-4)	13 (-7)	12 (-4)	14 (-1)	9 (-2)	5 (-3)	5 (-5)	9 (-5)	16 (-2)	20 (-2)	18 (-5)	16 (-6)	13 (-8)	11 (-7)	-
0*	41 (-2)	15 (0)	30 (-1)	17 (-3)	13 (-3)	13 (-2)	8 (-3)	5 (-3)	5 (-5)	9 (-5)	14 (-4)	17 (-5)	17 (-6)	15 (-7)	14 (-7)	13 (-5)	34 (-7)

Notes:
1. See Fig. 4.1 for location of readings
2. - indicates no reading taken
3. Number in parenthesis ( ) indicates change in reading from initial (zero load) reading
4. Positive number in parenthesis indicates eastward displacement
5. Negative number in parenthesis indicates westward displacement
6. * indicates readings were taken after the peak load was achieved (i. e. after failure)
7. Readings for load of 10000 lb. were taken when vertical deflection at midspan was 3.64"

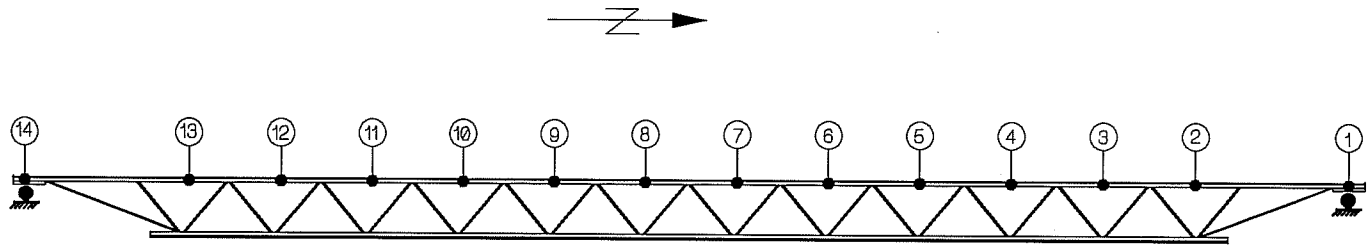

(a) Joist Nos. 1 and 2

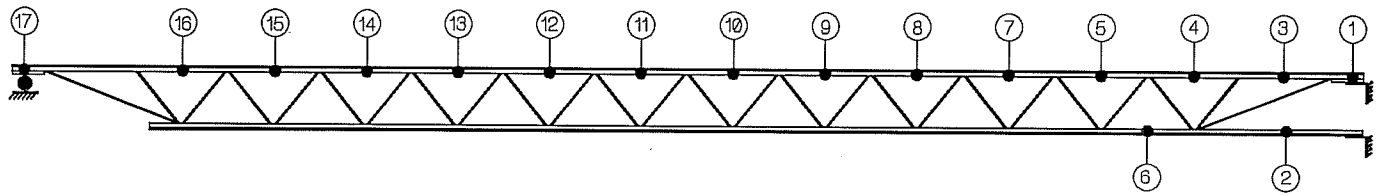

(b) Joist No. 3

Fig. 4.1 Locations of Transit Readings for Joist Lateral Displacements

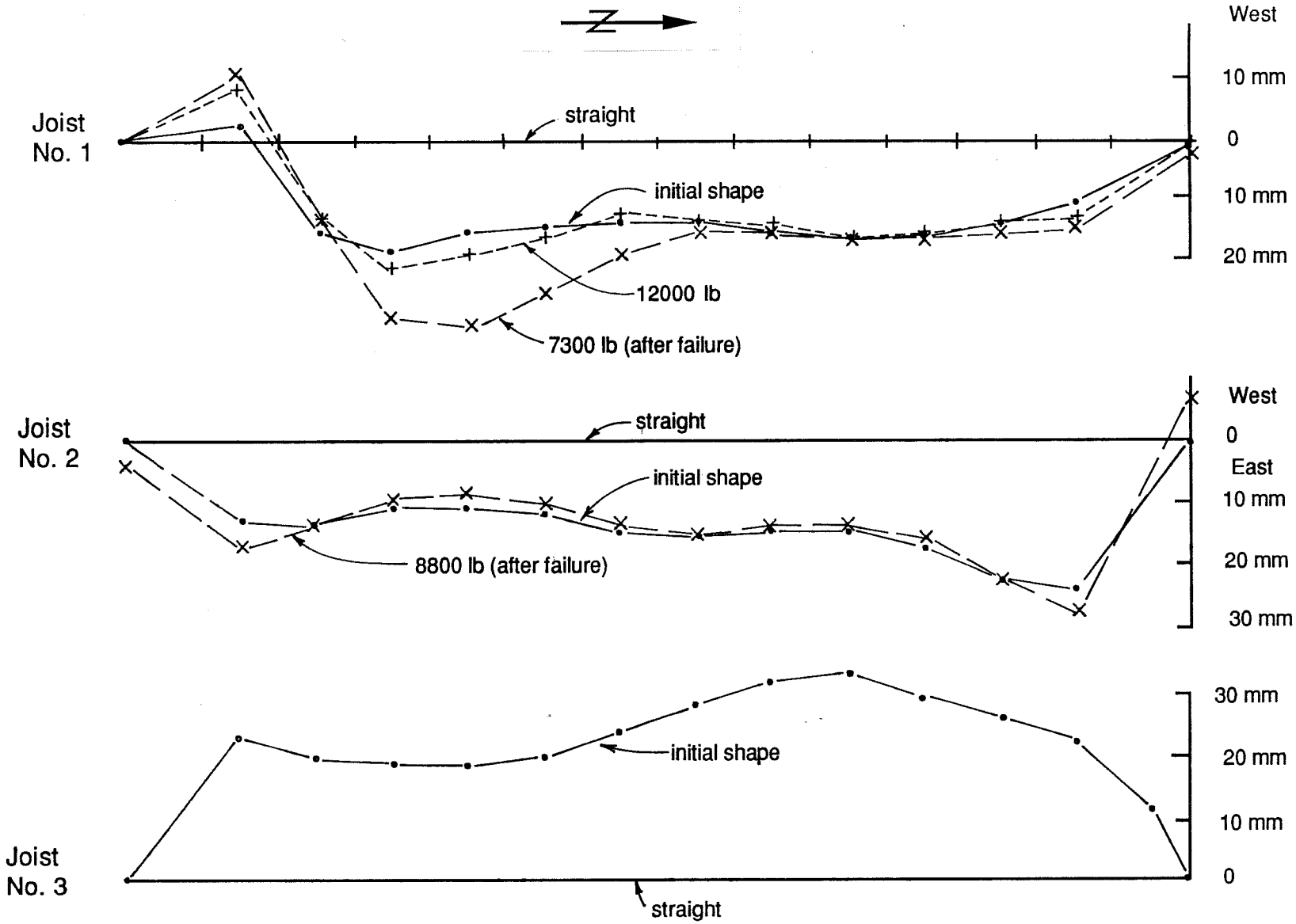

Fig. 4.1a Lateral Displacements of the Top Chord

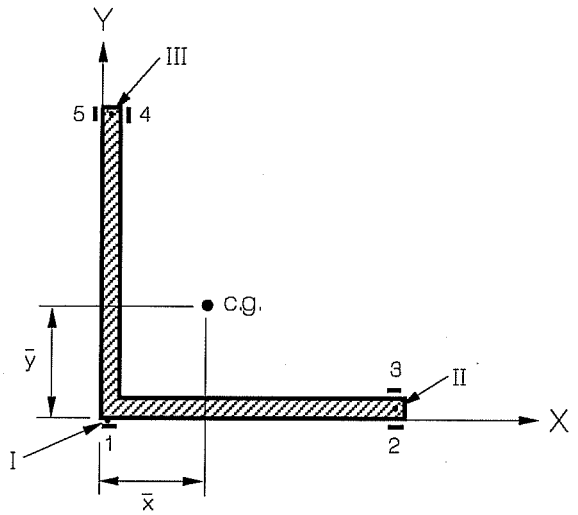

Typical Angle of Double Angle Chord Member

ϵ_1, ϵ_2, ϵ_3, ϵ_4, ϵ_5 = measured strains at strain gage locations

Compute: $\epsilon_I = \epsilon_1$
$\epsilon_{II} = (\epsilon_2 + \epsilon_3)/2$
$\epsilon_{III} = (\epsilon_4 + \epsilon_5)/2$

At any location (x, y), compute strain from: $\epsilon(x, y) = Ax + By + C$
where: A, B, C = constants

Solve for A, B, C from ϵ_I, ϵ_{II}, and ϵ_{III}, by solving system of three equations:
$\epsilon_I = \mathrm{A}\, x_I + \mathrm{b}\, y_I + \mathrm{C}$
$\epsilon_{II} = \mathrm{A}\, x_{II} + \mathrm{b}\, y_{II} + \mathrm{C}$
$\epsilon_{III} = \mathrm{A}\, x_{III} + \mathrm{b}\, y_{III} + \mathrm{C}$
where: (x_I, y_I) = coordinates of point I, etc.

Solve for $\bar{\epsilon}$ = strain at centroid of angle:
$\bar{\epsilon} = A\bar{x} + B\bar{y} + C$

For elastic response: $\bar{\sigma} = E\bar{\epsilon}$
where: $\bar{\sigma}$ = axial stress at centroid
E = 30,000 ksi.

Axial Force in angle = $\bar{\sigma} \times A_{angle}$
where: A_{angle} = cross-sectional area of angle

Total axial force in double angle member:
Repeat above calculations for other angle, and sum forces

Fig. 4.2 Computation of Axial Strain and Force in Double Angle Members

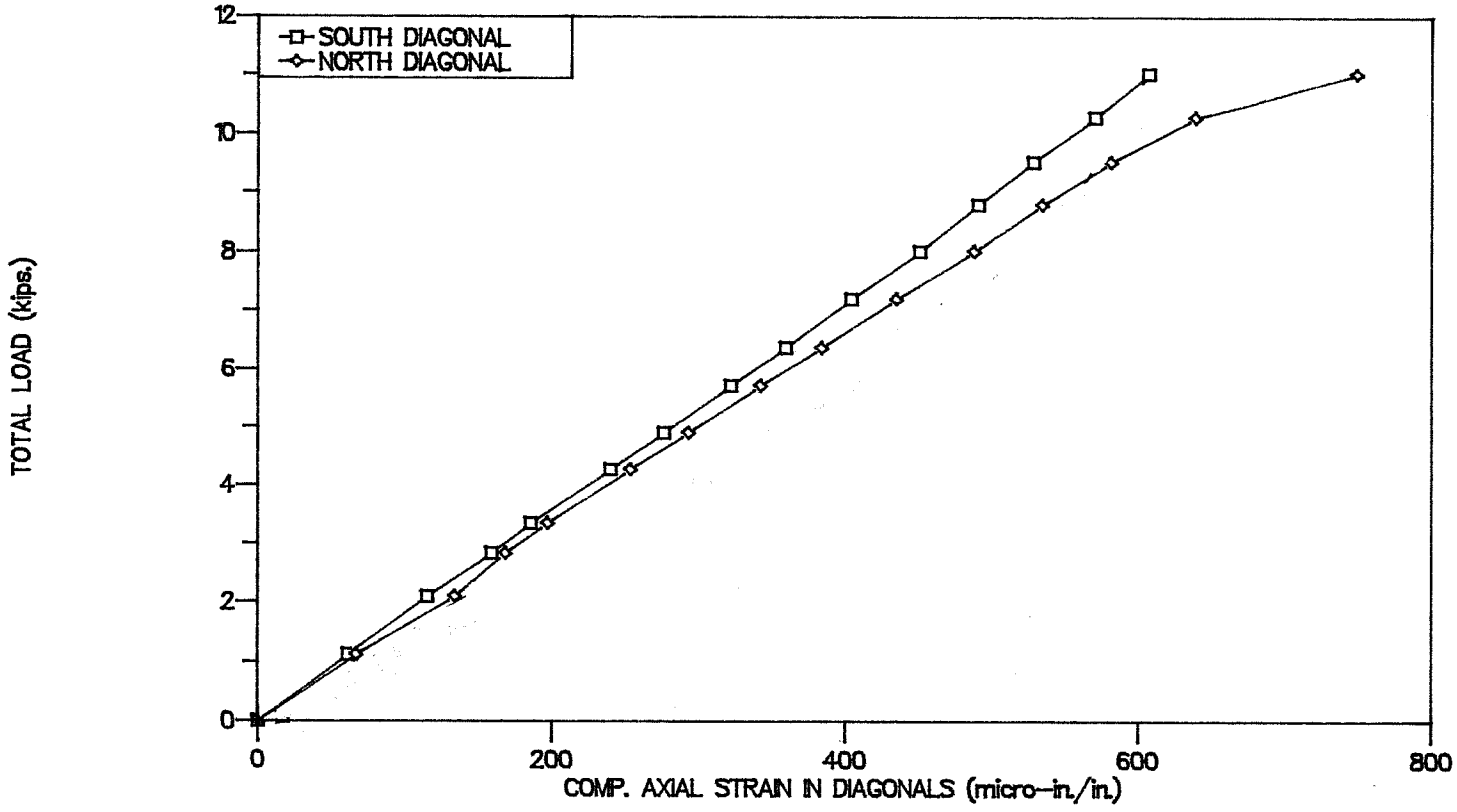

Fig. 4.3 Joist No. 2 – Estimated Axial Strain in Diagonals

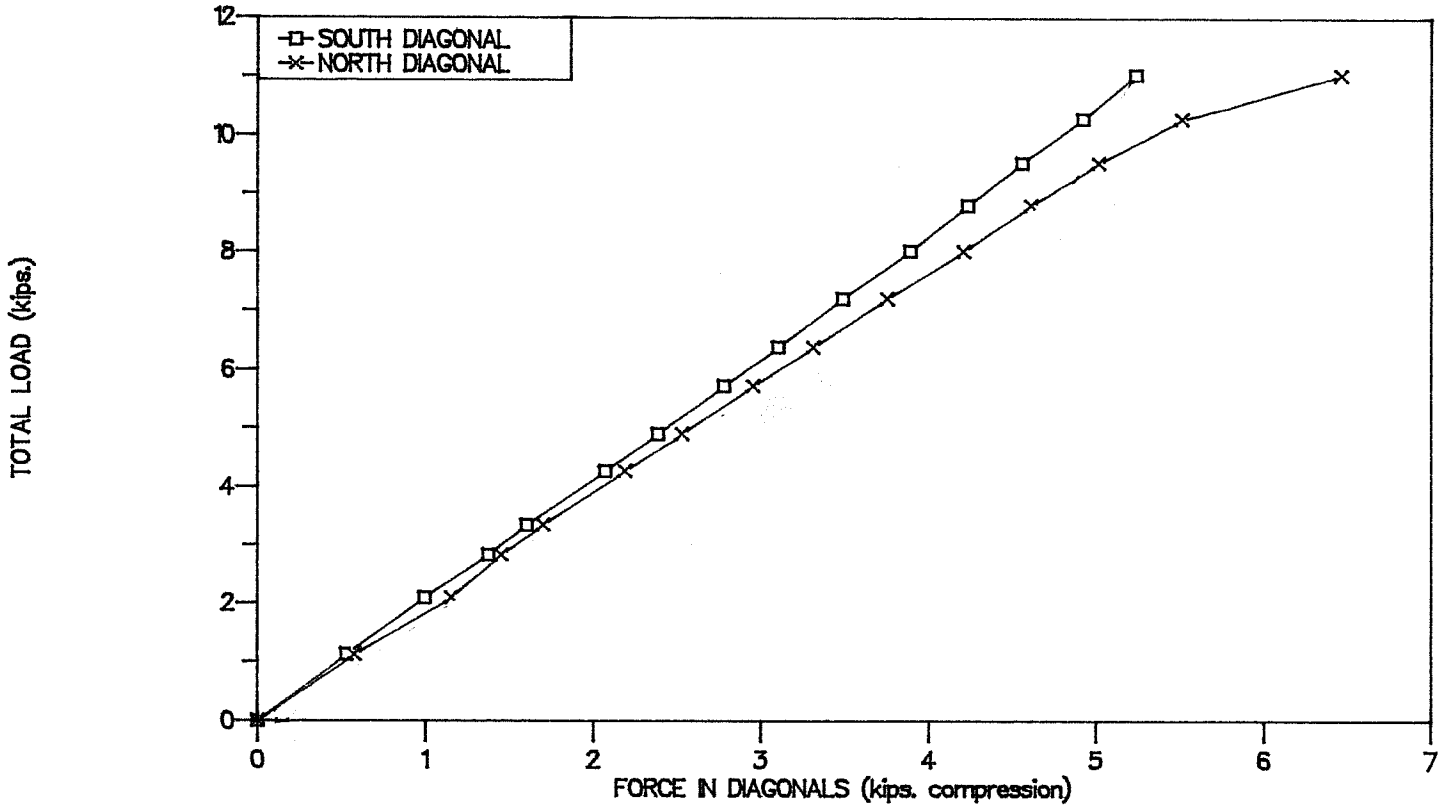

Fig. 4.4 Joist No. 2 – Estimated Axial Force in Diagonals

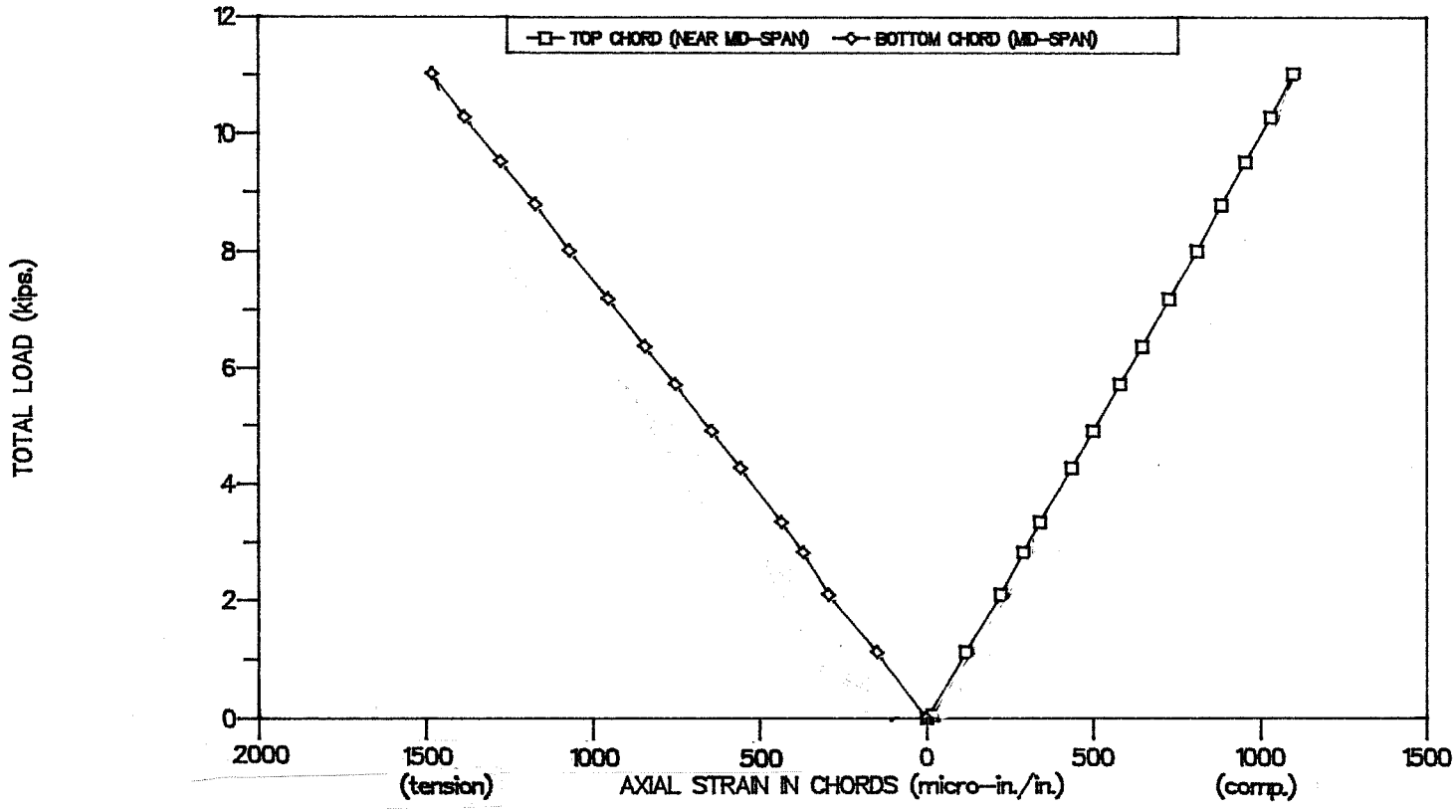

Fig. 4.5 Joist No. 2 – Estimated Axial Strain in Chord Members

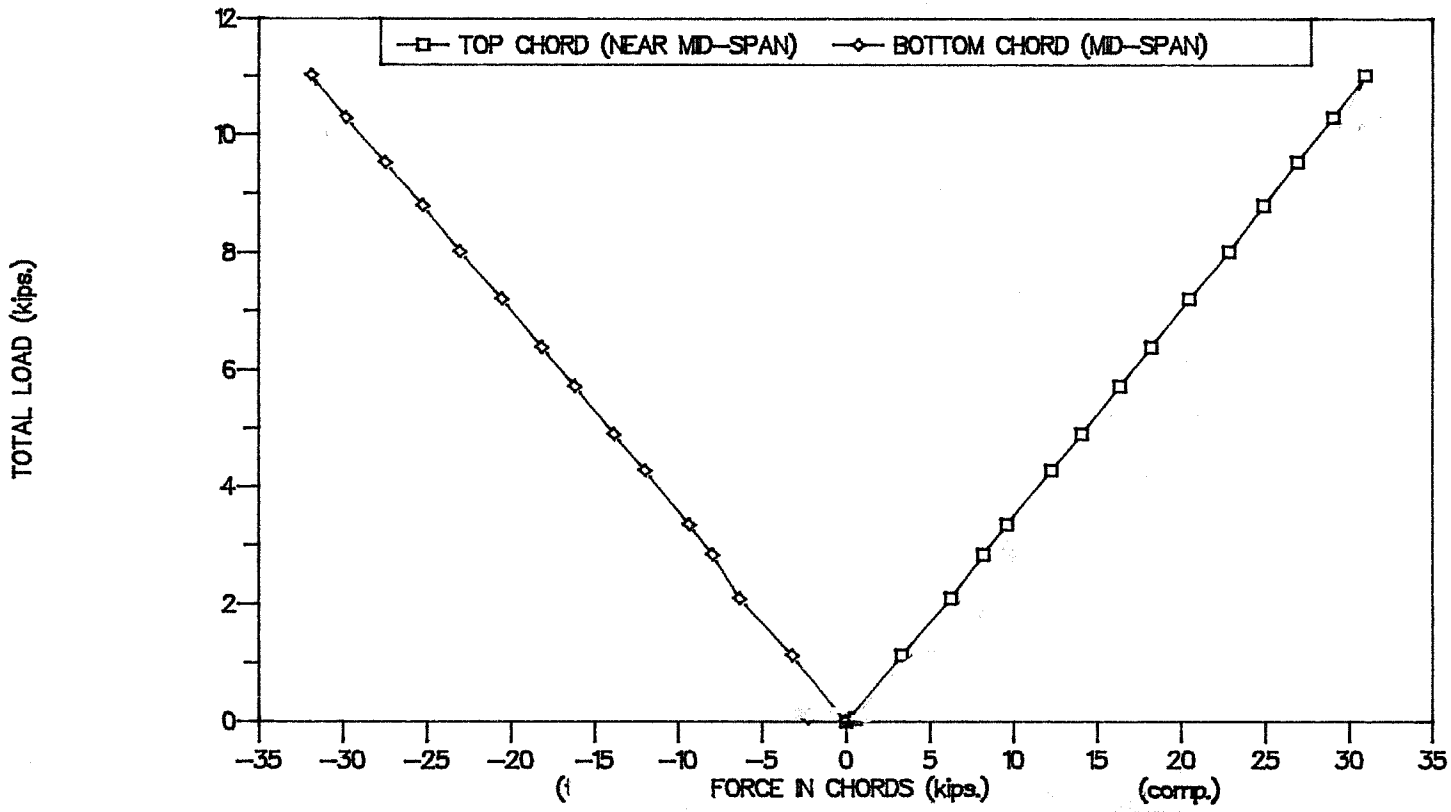

Fig. 4.6 Joist No. 2 – Estimated Axial Force in Chord Members

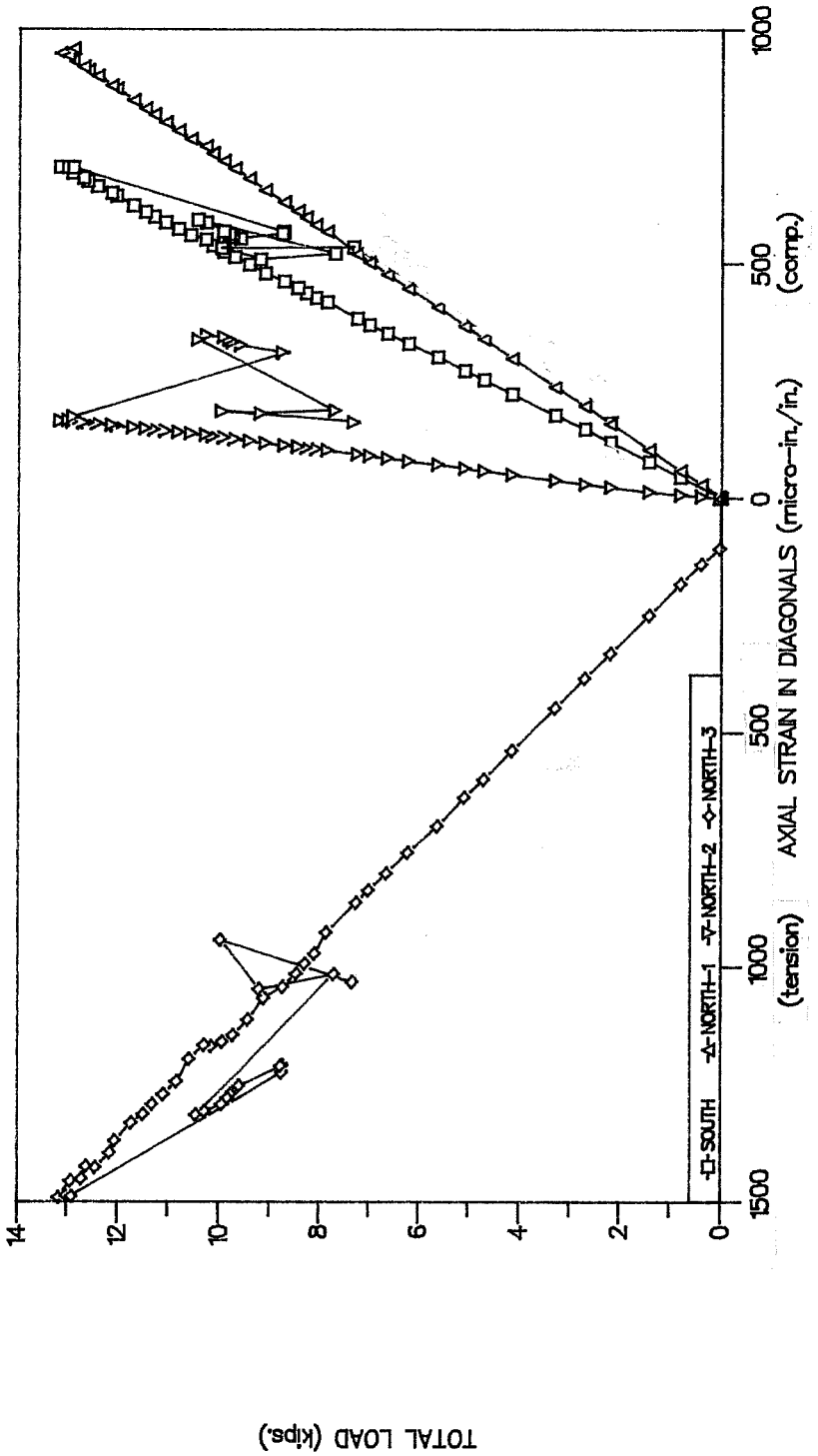

Fig. 4.7 Joist No. 3 – Estimated Axial Strain in Diagonals

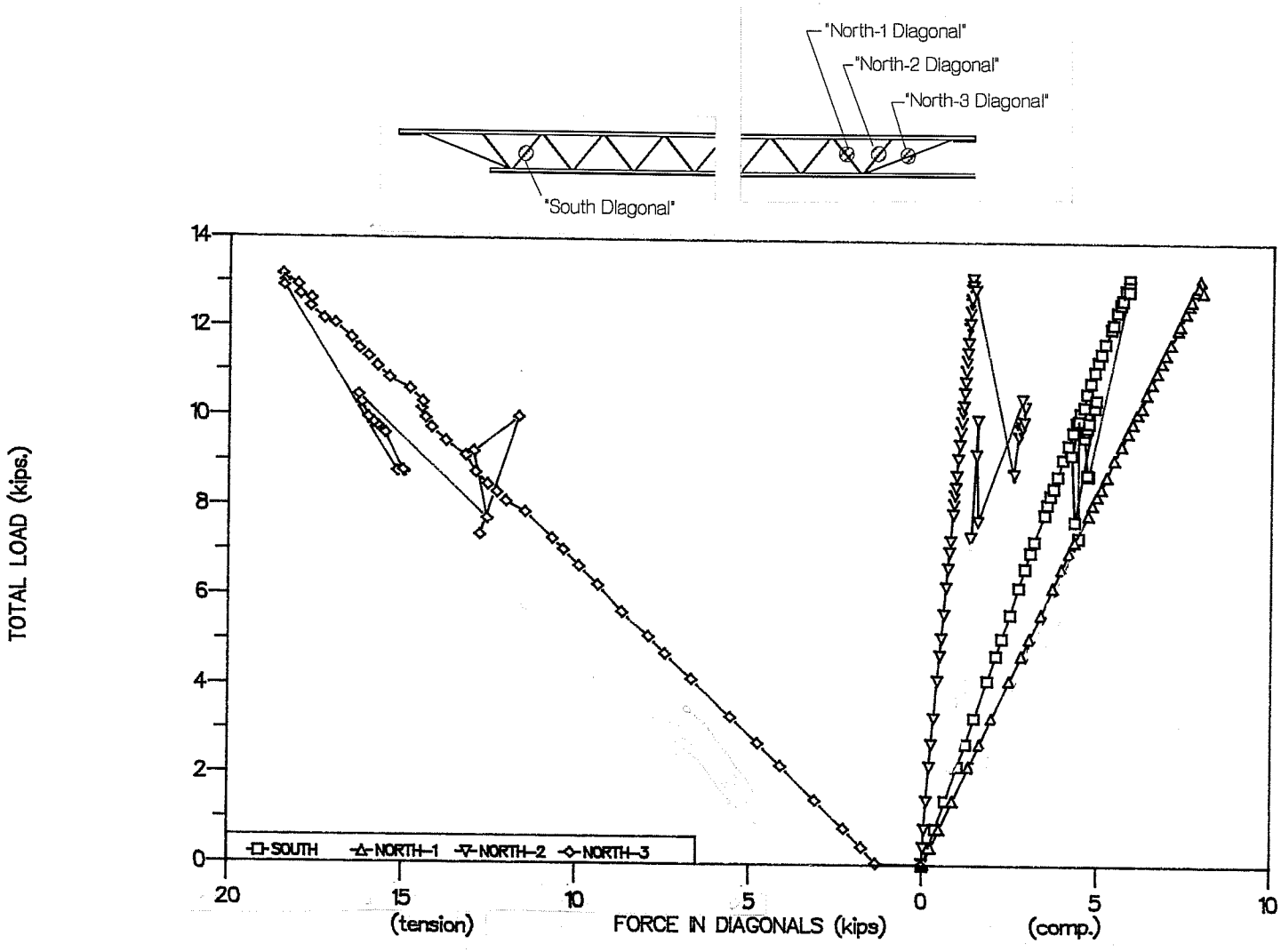

Fig. 4.8 Joist No. 3 – Estimated Axial Force in Diagonals

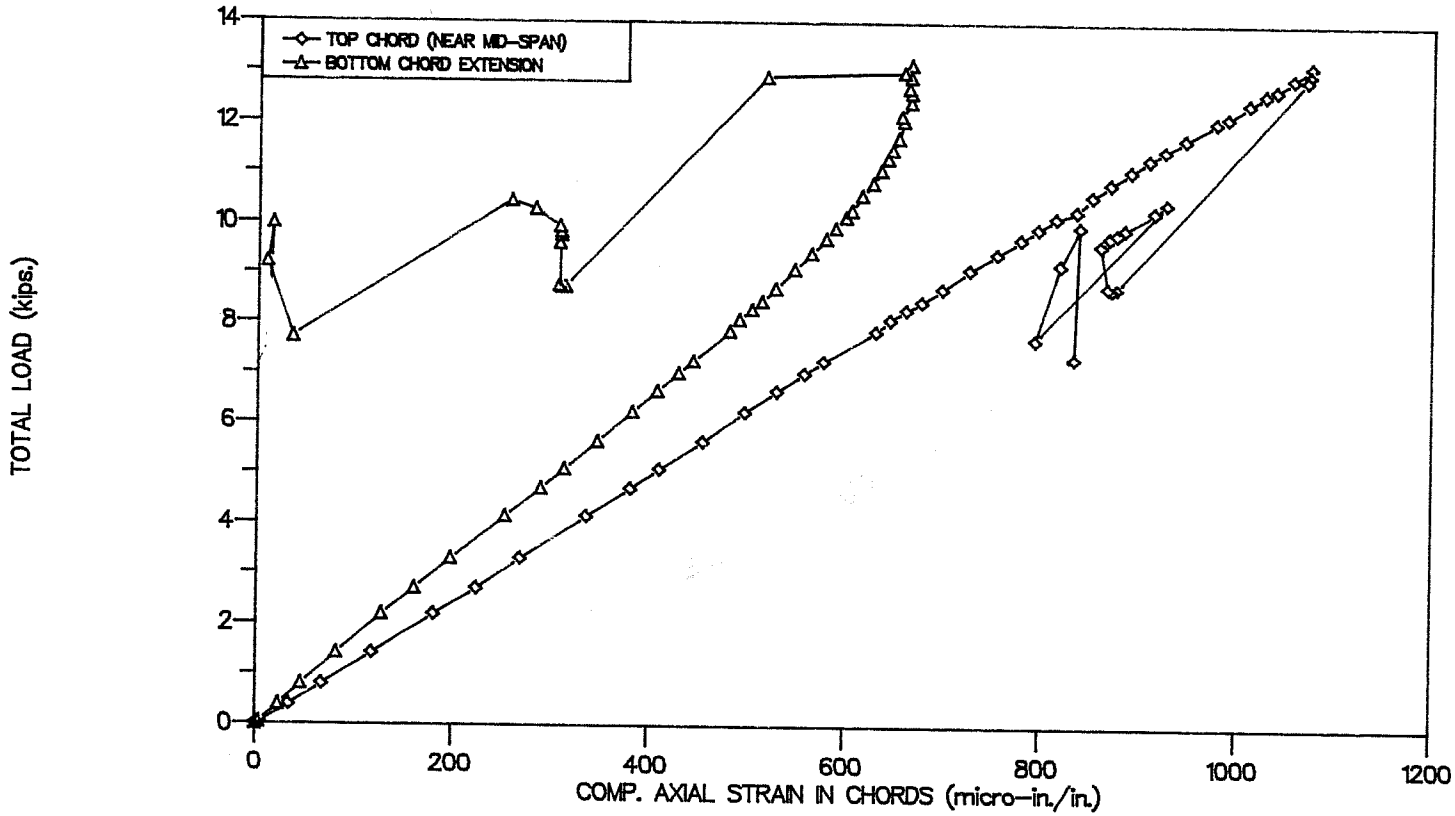

Fig. 4.9 Joist No. 3 – Estimated Axial Strain in Chord Members

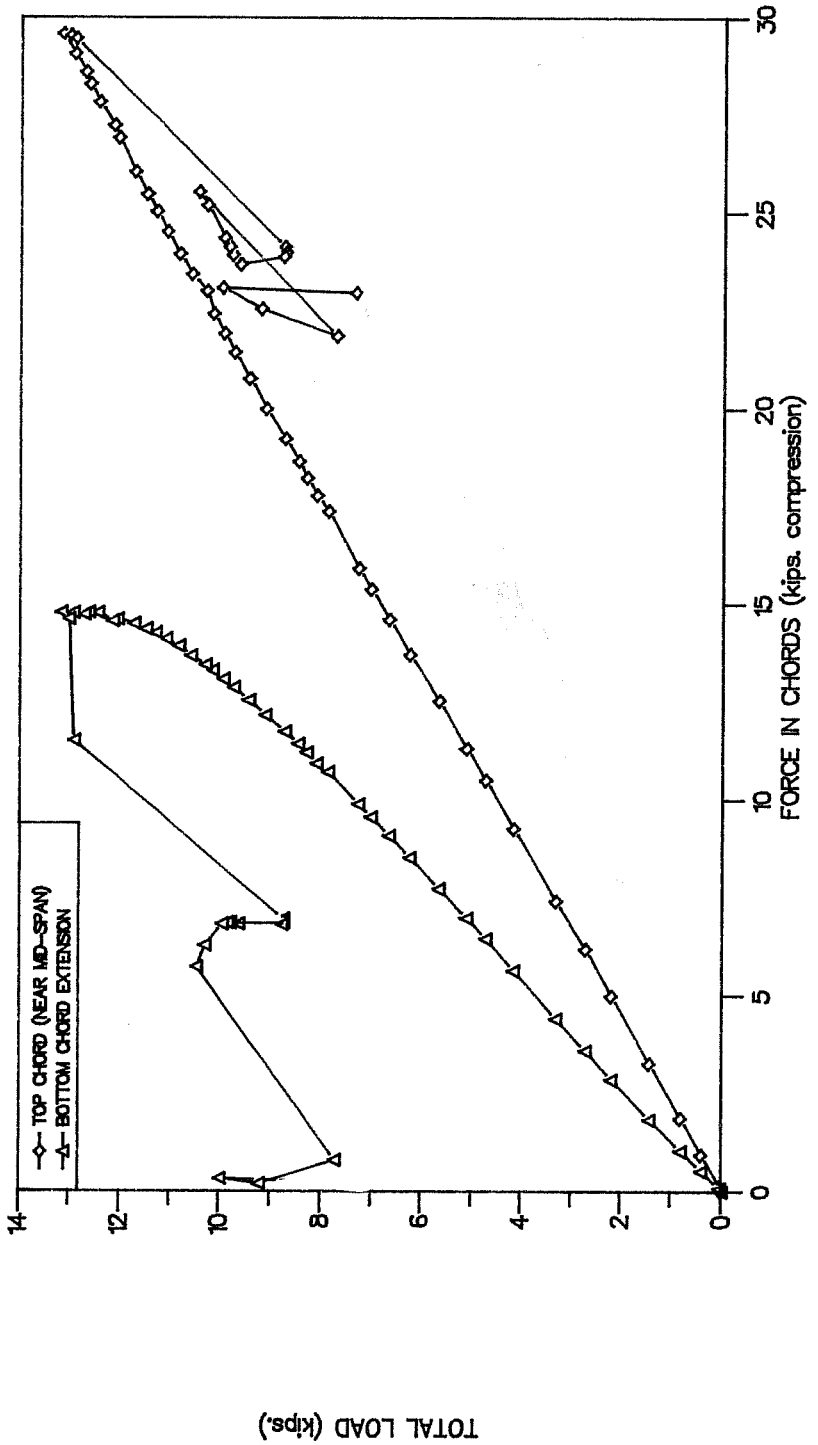

Fig. 4.10 Joist No. 3 – Estimated Axial Force in Chord Members